Multiband and Broadband impedance matching network

Nagaveni S

A Dissertation Submitted to
Indian Institute of Technology Hyderabad
In Partial Fulfillment of the Requirements for
The Degree of Master of Technology

भारतीय प्रौद्योगिकी संस्थान हैदराबाद
Indian Institute of Technology Hyderabad

Department of Electrical Engineering

December, 2014

Declaration

I declare that this written submission represents my ideas in my own words, and where others' ideas or words have been included, I have adequately cited and referenced the original sources. I also declare that I have adhered to all principles of academic honesty and integrity and have not misrepresented or fabricated or falsified any idea/data/fact/source in my submission. I understand that any violation of the above will be a cause for disciplinary action by the Institute and can also evoke penal action from the sources that have thus not been properly cited, or from whom proper permission has not been taken when needed.

_____

(Signature)

Nagaveni S

EE11M07

Approval Sheet

This Thesis entitled Broadband and Multiband Impedance Matching Networks by Nagaveni S. is approved for the degree of Master of Technology from IIT Hyderabad

Dr. Amit Acharyya) Examiner
Dept of _____ Eng
IITH

Dr. Sushmee) Examiner
Dept of _____ Eng
IITH

Dr. Asudeb Dutta) Adviser
Dept of _____ Eng
IITH

Dr. Shiv Govind Singh) Co-Adviser
Dept of _____ Eng
IITH

M.V.P. Rao) Chairman
Dept of CS Eng
IITH

iii

Abstract

This thesis proposes parasitic aware design techniques for concurrent Multi-Band impedance matching networks. Different concurrent L-matching networks are analyzed and the substantial impact of component non-idealities on matching performance is addressed. To counter these impacts, the design methodology is modified and the improvement is verified for different concurrent dual-band networks. The same techniques are extended for quad band concurrent L-matching networks. The proposed parasitic aware methods are validated through practical components from Coilcraft and Murata libraries (offchip) and UMC 0.18_um RFCMOS technology (on-chip). The results show considerable improvement in both off-chip and onchip scenarios. Hence, the proposed method is much useful in low power concurrent multi band RF circuit design.

The new methodology for broadband impedance matching has been discussed. In this the cascaded Highpass and Lowpass LC sections are designed at lower cutoff and Higher cutoff frequencies respectively. Bandwidth can be changed for given reflection coefficient. From this methodology a flat band is obtained.

In this document ,the parasitic impact on broadband impedance matching network is analyzed. In narrow band impedance matching the component parasitic degrades the matching performance. The impact of parasitic are significant hence parasitic aware techniques are introduced to improve the performance in real environment. In broadband impedance matching , the impact of parasitics are analyzed for different topologies using real and imaginary impedance equations. The observation made from this analysis is that, the impact of parasitic on broadband impedance matching is not significant.

Contents

1. Introduction

1.1   Introduction

The rapid growth in mobile technology and the consumer demands makes the mobile devices to be more compact, configurable, low power and low cost. In the present scenario, the modern mobile devices need to support multiple mobile standards like GSM900, DCS1800, UMTS2100 etc., and other short range communications like Bluetooth, WiFi, GPS, FM etc., as added services. To support multiple Radio Frequency (RF) standards in a single device, the inbuilt radio should be multi-band capable [1]-[4]. Multi-band performance can be realized by using either of i) multiple narrow-band, ii) configurable narrow-band iii) wide-band iv) concurrent multiband hardware. The configurable narrow-band network is incapable, when multiple standard connectivity is needed simultaneously. As an example, an on the drive map utility needs GPS connectivity for position information and WiFi or GPRS for map data [5]. Moreover, the reconfigurable architecture reduces the sensitivity of the receiver. The wide-band network shows poor performance in a case, where stronger out of band blockers exist. The multiple narrow-band needs complex hardware which leads large chip area and hence high cost. On the other hand, concurrent multi-band system overcomes all these negatives and will be most suitable for multi-standard radio implementation [6]-[9].

In concurrent multi-band circuit, the input reflection must be minimized to achieve maximum power transfer from source to load and thus better overall performance. Passive impedance matching is a key way for achieving this in low power RFIC design perspective [10], [11]. Low Noise Amplifier (LNA) input impedance matching and antenna impedance matching are the specific matching requirement in receiver and transmitter respectively. In concurrent multi-band RF circuits, the matching has to be achieved all the required bands simultaneously to reduce reflection. There are different approaches proposed in literatures for concurrent dual band matching, like L-match, PI-match and T-

1

match and each network can be bandpass or bandstop nature [12], [13] . A generic design approach for multi-band concurrent matching network design is introduced in [13]. In all the design approaches, the passive components are taken as ideal and their parasitic impacts were never addressed. But the quality factor of the on-chip passives are in the range of ten, which leads to considerable impact by the parasitics associated with them. Impacts of component non-idealities in RF circuits and the need of parasitic aware design is presented in [14]. Recent literatures [15]-[17] proposed dynamic and adaptive tuning of component values for better matching performances. However, to achieve the dynamic matching, the additional complex control mechanism is required. This control algorithm may be implemented in on-chip or software control with external interfaces. In such cases, the complete system need more hardware and software resources and the design will be more time consuming. Hence, there is a need of generic analytical approach for designing multi-band concurrent matching networks accounting their inherent parasitics in the design phase itself.

1.2　Aim and Motivation

Modern mobile handsets need to support multiple wireless standards like GSM, UMTS, Bluetooth, GPS, WLAN, as well as FM. Each of these standards are specified at different frequencies and moreover, standards such as GSM and UMTS themselves are specified for different frequency bands in different regions of the world. This requires a handset to be capable of supporting multiple radio frequencies. Users of mobile handsets routinely use 2–3 services/radios at the same time. For example, a scenario where a user would use GPS for location services, data services to access maps, and Bluetooth services to pair a headset while driving, can easily be imagined. In handsets that are available in the market, multiple radios are supported by dedicated hardware for each radio. This is a sub-optimal solution in terms of hardware sharing and power consumption. Reconfigurable circuits are used
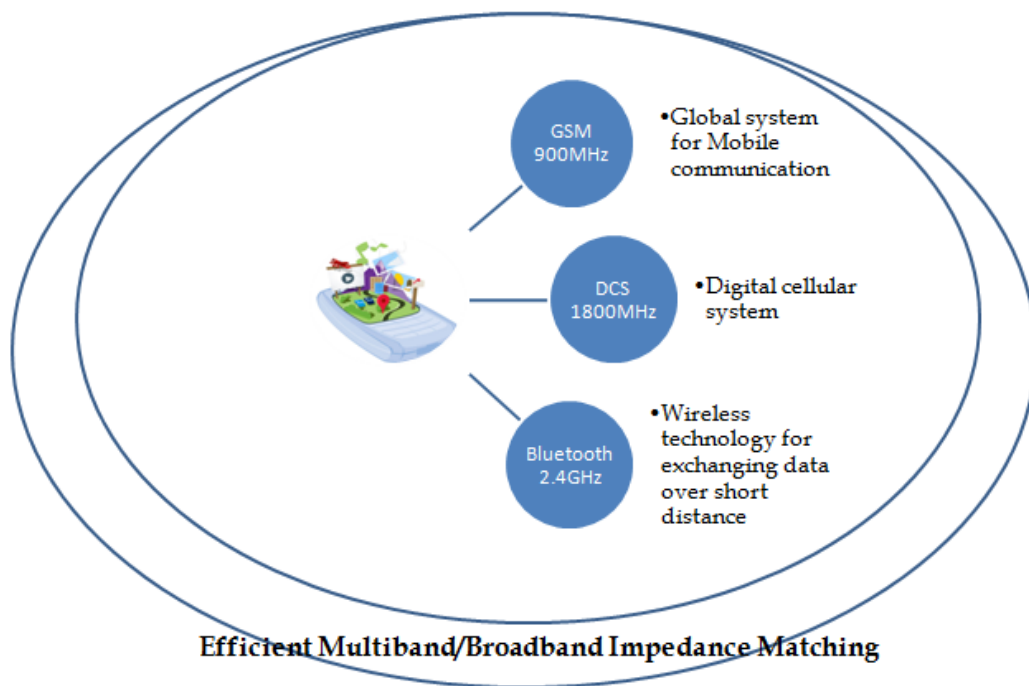
Figure 1.1 . Aim and Motivation.

1.3   Literature Survey

Reconfigurable circuits are used to support multiple frequencies, but not at the same time. Moreover, in general, reconfigurability is achieved by switches which, at the RF front-end reduce the sensitivity of the receiver [12]–[14]. One can also use wide-band circuits to support multiple standards [15]–[18], but requires a careful frequency planning and filtering as the number of interferers are high. An alternate architecture which can potentially overcome all the above mentioned challenges has been suggested in [19]. This architecture, makes it possible to share a single LNA/PA by multiple radio systems through the use of switch-less multi-band matching networks [20]–[24]. Several multi-band matching networks have been reported in the recent past [25]–[31]. Among these, [28]–[31] discuss only the design of dual-band matching networks. [25], [26] are based on cascading of L-match networks (composed of distributed and/or lumped elements) tuned to different frequencies. [27] is a multi-band matching

3

network using transmission lines, and solves a system of non-linear equations with a set of given constraints. All of the above methods increase in complexity as the number of bands increases. Further, little intuition is gained as far as circuit design is concerned.

1.4   Contribution of Thesis

This work focuses on the design of systematic and generic impedance matching networks for RF front end. The main contributions of this research work are as follows:

- A generic and systematic techniques Equivalent impedance method and parasitic absorption method for designing multiband impedance matching including component parasitic are proposed.
- Discussed new method for designing Broadband impedance matching networks which provides uniformity over a band.
- Mathematically analyzed the impact of component parasitics on broadband impedance matching.

2. Concurrent   Multi-band   Impedance Matching

2.1   Introduction

The design of concurrent dual band L-matching network is derived from simple narrow band L-matching network. The type of L-matching network can be any of the possible four circuits.
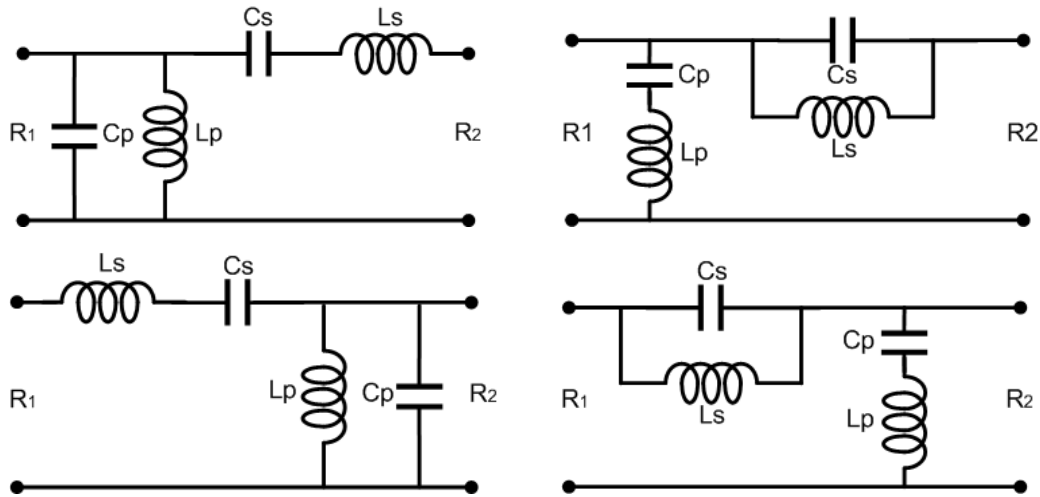
Fig. 2.1. Concurrent Dual-Band L-match Networks

1) Low Pass High to Low (LP-HtoL)

2) Low Pass Low to High (LP-LtoH)

3) High Pass High to Low (HP-HtoL)

4) High Pass Low to High (HP-LtoH)

Hence the transformed band pass circuit for concurrent operation will also be in four categories. The possible concurrent dual band circuits derived from narrow band L-match circuits are shown in Fig. 1. In need of multiple degrees of freedom (circuit quality factor and transformation ratio), the Pi and T-matching works are also being used. However, by the benefit of circuit simplicity and less number of components, L-matching networks are more preferred [18]-[19]. Therefore this document emphasizes on concurrent multi-band L-matching networks. Matching performance of the networks degrade due to the inherent parasitics of passive components and are noticed in literatures [6], [13]. To get an insight of that, we have analyzed the impact of component non-idealities and the modified methods to improve the performance are addressed in the following section.

2.2 Parasitic Aware Technique For Concurrent Dual-Band Network

Parasitic Impact on Matching Performance The design methods briefed in literatures provide a good matching performance when the components are ideal (Q =1). In the real scenario, component quality factors are always finite and even too low values in on-chip case. These parasitic will impact the circuit performance in terms of matching quality and matching frequency. As example, a concurrent dualband band-pass high to low (CC-DB-BP-HtoL) L-matching network is detailed below. The series parasitic resistance associated with inductor and capacitor can be written in terms of their quality factor as shown below (1).

$$R_L = \frac{X_L}{Q_L} \qquad , \qquad R_C = \frac{X_C}{Q_c} \tag{1}$$

Table I lists the derived component values for matching from 500Ω load to 50Ω source impedance in ideal case. Matching performance (in terms of input reflection coefficient S11) of the circuit with the tabulated component values are plotted in ideal case and two different quality factor cases and are shown in Fig. 2. From the figure, it is clear that the parasitic impact

Table I
Component values for cc-db-bp l-matching network for
R1 = 50, R2 = 500.

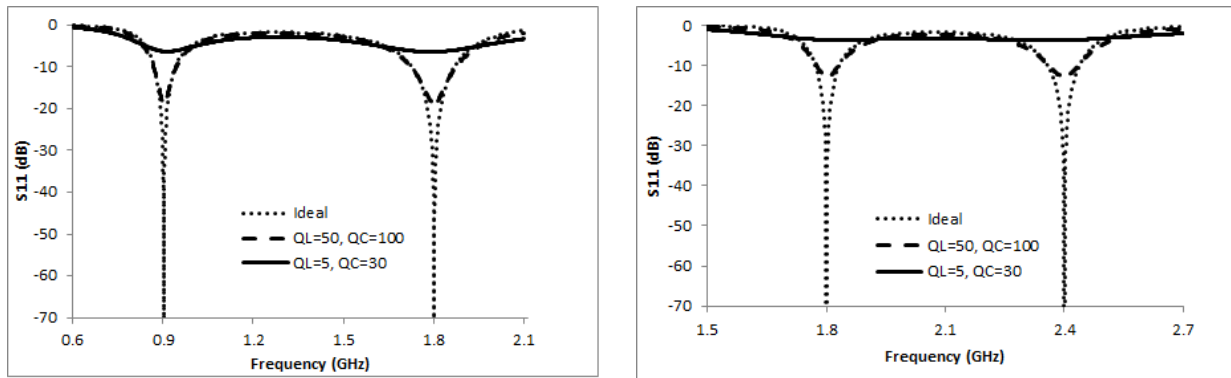| f1,f2 (GHz)	Ls (nH)	Cs (pF)	Lp (nH)	Cp (pF)
0.9, 1.8	26.5	0.59	14.7	1.06
1.8, 2.4	39.8	0.15	3.68	1.59

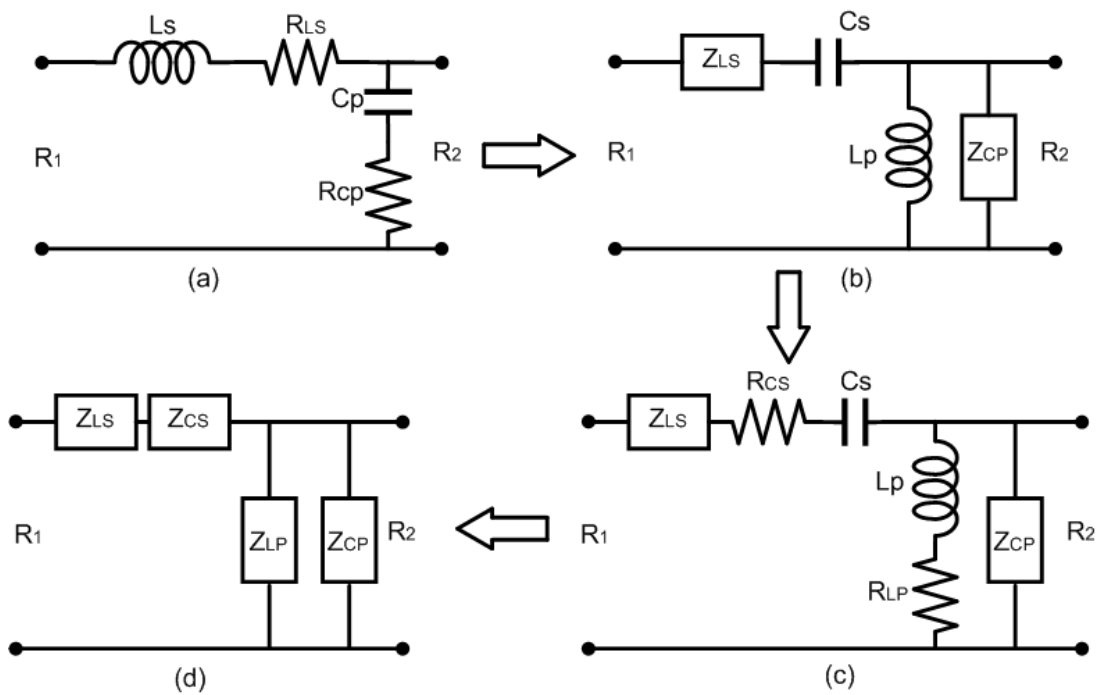Fig. 2.2 Parasitic Impact of Non-ideal components in Matching Network

Fig. 2.3. Transformation of ideal to real L-matching and Concurrent Dual Band Matching Circuit

is prominent and is even crucial in on-chip case. Hence, the parasitic impacts should be accounted in the design phase for achieving better matching performance. For this, in the below subsections, we propose two parasitic aware design methods for designing concurrent dual-band matching networks.

7

2.2.1. Equivalent Impedance Method

The ideal CC-DB-BP-HtoL L-matching circuit and its step by step transformation into parasitic aware concurrent band pass circuit is shown in Fig. 3. The proposed design approach is explained in two steps. In first, a narrow band low pass L-matching (LP-HtoL) network components (LS and CP) are designed using parasitic aware L-matching technique [20] and the rest two components (LP and CS) are derived form the total impedance equation (including component parasitics). In second step, using the above derived component values (LP and CS), the initial L-matching (LS and CP) components are recalculated for better performance. The derivation followed by a design example is explained below.

1) Step-1: In the first step of the proposed approach, the narrow band low pass L-matching network is derived using parasitic aware method as given in [20] to calculate the initial two components LS and CP . The input impedance of the Lmatching circuit including the component parasitic is

$$\frac{1}{R_1} = \frac{1}{R_2 + jX_{Ls} + \frac{X_{Ls}}{Q_L}} + \frac{1}{\frac{X_{cp}}{Q_c} - jX_{cp}} \tag{2}$$

By separating the real and imaginary part of the load impedance and equating it to its source counterpart, the following quadratic equations were obtained

$$X_{Ls}^2 \left(1 + \frac{1}{Q_L^2}\right) + X_{Ls} \left(\frac{2R_2}{Qc} + R1 \left(\frac{1}{QL} + \frac{1}{Qc}\right)\right) - R_2^2 Q^2 = 0 \tag{3}$$

$$X_{cp}^2 \left(1 + \frac{1}{Q_c^2}\right) + X_{cp} \left(\frac{Q^2 + 1}{Q^2}\right) \left(\frac{2R_2}{QL} - R1 \left(\frac{1}{QL} + \frac{1}{Qc}\right)\right) - \frac{R_1^2}{Q^2} = 0 \tag{4}$$

Where $Q = \sqrt{1 - \frac{R1}{R2}}$ s system quality factor

8

By solving (3) and (4), the component values for narrow band L-matching network including their parasitics are calculated for the frequency $w01 = w1 - w2$. Then, this parasitic aware narrow band LP L-matching network is converted into CC-DB-BP network using the frequency transformation method given in [13]. And the remaining two components are derived by accounting their parasitics through equivalent impedance method.

In this, the impedance equation for the complete circuit is derived including load impedance and all component parasitic. Then it is solved for the two unknown components (LP and CS) at frequency $w_{02} = \sqrt{w_1 w_2}$. The complete derivation are presented in detail below.

Considering all the parasitic, the input impedance of the circuit becomes,

$$R_1 = jXLs + \frac{XLs}{QL} - jXcs + \frac{Xcs}{Qc} + \cfrac{1}{\cfrac{1}{R_2} + \cfrac{1}{jXLp + \cfrac{XLp}{QL}} + \cfrac{1}{-jXcp + \cfrac{Xcp}{Qc}}} \quad (5)$$

By splitting real and imaginary part of the input impedance and equating those to their source impedance counterpart leads to two quadratic equations as given below.

The value of XLP and hence LP can be found by solving the quadratic equation (6)

$$X_{Lp}{}^2(pr - km) + X_{Lp}(ps + qr - kn - lm) + (qs - \ln) = 0 \quad (6)$$

Where

$$
\begin{aligned}
p &= -R_1 X_{cp} - \frac{R_1 X_{cp}}{Q_c Q_L} - \frac{R_1 R_2}{Q_L} + R_2 X_{Ls}\left(\frac{1}{QL^2} - 1\right) + X_{Lp}X_{cp}\left(\frac{1}{Q_L} - \frac{1}{Qc}\right) \\
&\quad + \left(\frac{X_{Ls}X_{cp}}{Q_L} + R_2 X_{cp}\right)\left(1 + \frac{1}{Q_L Q_c}\right)
\end{aligned} \quad (7)
$$

$$q = -\frac{R_1 R_2 X_{cp}}{Qc} + R_2 X_{Ls} X_{cp}\left(1 + \frac{1}{Q_L Q_c}\right) \quad (8)$$

$$r = \left(R_2 + \frac{X_{cp}}{Qc}\right)\left(\frac{1}{Q_L} - \frac{1}{Qc}\right) + X_{cp}\left(1 + \frac{1}{Q_LQ_c}\right) \tag{9}$$

$$s = \frac{2R_2Xcp}{Qc} \tag{10}$$

$$k = -\frac{Xcp}{Qc}\left(2 + \frac{1}{QLQc}\right) + \frac{Xcp}{QL} - R_2 \tag{11}$$

$$l = R_2X_{cp}\left(1 - \frac{1}{Qc}\right) - \frac{R_2X_{Ls}}{QcQL} \tag{12}$$

$$m = \left(\frac{X_{Ls}X_{cp}}{QL} + X_{cp}R_2\right)\left(\frac{1}{Qc} - \frac{1}{QL}\right) - X_{cp}R_1\left(\frac{1}{Qc} + \frac{1}{QL}\right) - R_1R_2 + \frac{2R_2X_{Ls}}{QL} + X_{Ls}X_{cp}\left(1 + \frac{1}{Q_LQ_c}\right) \tag{13}$$

$$n = R_2X_{Ls}X_{cp}\left(\frac{1}{Qc} - \frac{1}{Q_L}\right) + R_1R_2X_{cp} \tag{14}$$

Calculation of XCS and thus CS is also derived in a similar fashion by solving the quadratic equation (15)

$$X_{cs}{}^2(pr - km) + X_{cs}(ps + qr - kn - lm) + (qs - \ln) = 0 \tag{15}$$

Where,

$$p = \frac{R_2X_{cp}}{Qc^2} + \frac{R_2X_{Ls}}{QLQc} - X_{cp}R_2 \tag{16}$$

$$q = \frac{R_2}{Qc}\left(-R_1X_{cp} + \frac{X_{Ls}X_{cp}}{QL}\right) + X_{cp}R_2X_{Ls} \tag{17}$$

$$r = X_{cp}\left(1 - \frac{1}{Q_c^2} + \frac{2}{Q_LQc}\right) + R_2\left(\frac{1}{QL} - \frac{1}{Qc}\right) \tag{18}$$

$$s = R_1X_{cp}\left(\frac{1}{Qc} - \frac{1}{QL}\right) + R_1R_2 + \frac{X_{Ls}X_{cp}}{QL}\left(\frac{1}{QL} - \frac{1}{Qc}\right) - \frac{2R_2X_{Ls}}{QL} + R_2X_{cp}\left(\frac{1}{QL} - \frac{1}{Qc}\right) - X_{Ls}X_{cp}\left(1 + \frac{1}{QLQc}\right) \tag{19}$$

$$k = -\frac{2R_2X_{cp}}{Qc} \tag{20}$$

$$l = R_2 X_{cp}\left(R_1 - \frac{X_{Ls}}{Q_L}\right) + \frac{R_2 X_{cp} X_{Ls}}{QL} \tag{21}$$

$$m = -\frac{X_{cp}}{Qc}\left(1 + \frac{1}{Q_L Qc}\right) + X_{cp}\left(\frac{1}{QL} - \frac{1}{Qc}\right) - R_2 \tag{22}$$

$$\begin{aligned}
n &= \left(R_1 X_{cp} - R_2 X_{cp} - \frac{X_{Ls} X_{cp}}{QL}\right)\left(1 + \frac{1}{Q_L Qc}\right) + \frac{R_1 R_2}{QL} + R_2 X_{Ls}\left(1 - \frac{1}{Q_L^2}\right) \\
&\quad + X_{Ls} X_{cp}\left(\frac{1}{Qc} - \frac{1}{QL}\right)
\end{aligned} \tag{23}$$

Table II
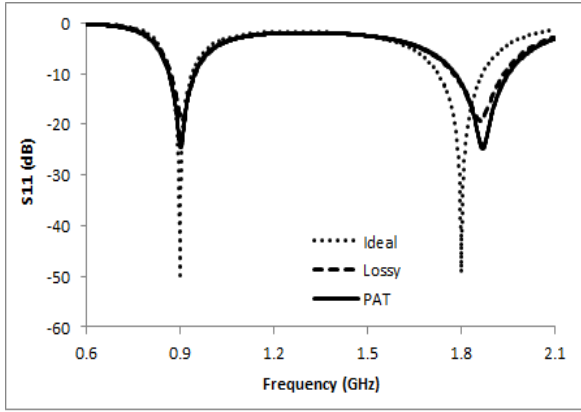Derived component values in step.1 of equivalent impedance
Method for cc-db-bp network.

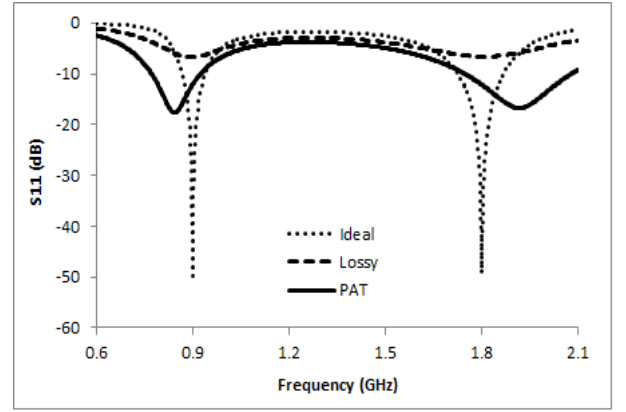| QL, Qc	H to L (500Ω to 50Ω)				L to H (5Ω to 50Ω)			
	Ls (nH)	Cs (pF)	Lp (nH)	Cp (pF)	Ls (nH)	Cs (pF)	Lp (nH)	Cp (pF)
∞, ∞	26.5	0.59	14.8	1.06	2.65	5.9	1.48	10.6
50, 100	24.6	0.63	13.2	1.17	2.62	5.73	1.61	9.3
5, 30	17.4	0.89	6.26	2.49	3.64	4.12	2.99	5.01

(a) High to Low: Off-Chip

(b) High to Low: On-Chip

11
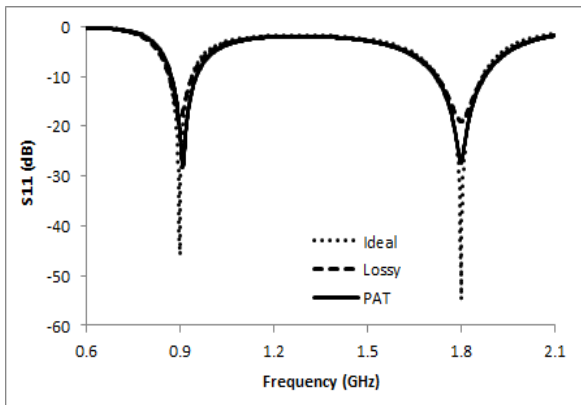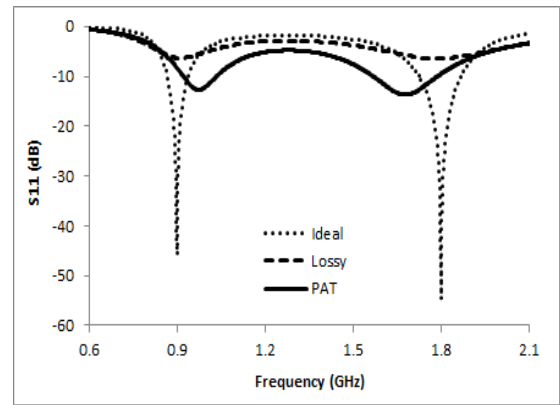
(c) Low to High: Off-Chip   (d) Low to High: On-Chip

Fig. 4. S11 response of CC-DB-BP L-matching Networks with derived
components using Step.1 of Equivalent Impedance method

Using equations (3), (4, (6) and (15) the component values are derived for 500to50
matching in different quality factors. The same method is extended for low to high (5
to 50) matching network as well. The component values calculated for 0.9GHz and
1.8GHz in these two cases are listed in Table II.

The S11 plots of the L-matching circuits using these component values are shown
in Fig. 4. From the Fig. 4 it is clear that, the proposed parasitic aware concurrent
dual-band design approach (stpe-1) improves the matching performance.

Though this method gives improved matching performance as compared to
lossy components performance, a frequency drift is observed. To overcome this
issue, the derivation procedure is extended in Step-2, where LS and CP are
recalculated again with respect to overall system perspective (total impedance), as
described below.

2) Step:2: In this step, the solution for initial components (LS and CP) are
   derived again from the overall impedance equation by substituting the pre-
   calculated LP and CS.

For this, the real and imaginary part of overall impedance equation given in (5) is
splitted. Equating these with their source impedance counterpart, two quadratic

12

equations are derived for the two unknown variables (LS and CP), as given in (24) and (33). The complete derivation is given below.
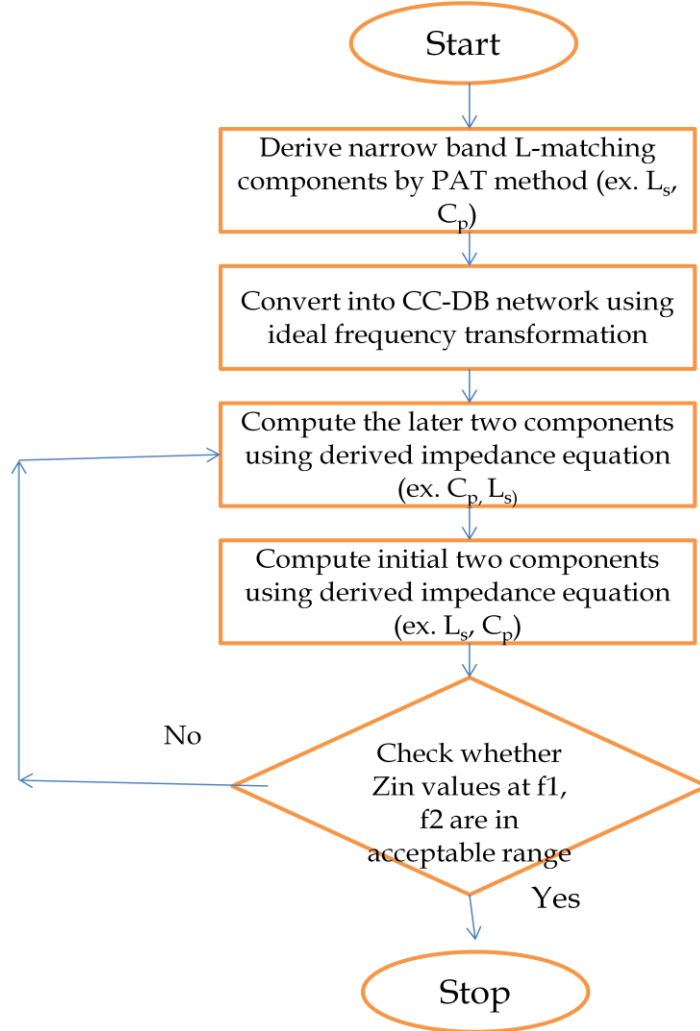

Fig. 5. Equivalent Impedance method Flow Chart

$$X_{Ls}{}^2(pr - km) + X_{Ls}(ps + qr - kn - lm) + (qs - \ln) = 0 \qquad (24)$$

Where

$$p = \left(-R_2 - \frac{X_{Lp}}{QL}\right)\left(1 + \frac{1}{Q_L Q_c}\right) + X_{cp}\left(\frac{1}{Q_L} - \frac{1}{Qc}\right) \qquad (25)$$

13

$$q = \left(R_1 X_{Lp} - \frac{X_{cs} X_{Lp}}{Q_L} - R_2 X_{Lp}\right)\left(1 + \frac{1}{Q_L Q_c}\right) + \frac{R_1 R_2}{Q_c} - R_2 X_{cs}\left(\frac{1}{Q_c^2} - 1\right)$$
$$+ X_{Lp} X_{cs}\left(\frac{1}{Q_L} - \frac{1}{Q_c}\right) \tag{26}$$

$$r = R_2 X_{Lp}\left(\frac{1}{Q_L^2} - 1\right) - \frac{R_2 X_{cs}}{Q_c Q_L} \tag{27}$$

$$s = R_2 X_{Lp}\left(X_{cs} - \frac{R1}{Q_L}\right) \tag{28}$$

$$k = (R_2 + \frac{X_{Lp}}{Q_L})\ \left(\frac{1}{Q_c} - \frac{1}{Q_L}\right) - X_{Lp}\left(1 + \frac{1}{Q_L Q_c}\right) \tag{29}$$

$$l = \left(\frac{X_{cs} X_{Lp}}{Q_c} + X_{Lp} R_2\right)\left(\frac{1}{Q_L} - \frac{1}{Q_c}\right) - X_{Lp} R_1\left(\frac{1}{Q_L} + \frac{1}{Q_c}\right) - R_1 R_2 + \frac{2 R_2 X_{cs}}{Q_L}$$
$$+ X_{cs} X_{Lp}\left(1 + \frac{1}{Q_L Q_c}\right) \tag{30}$$

$$m = \frac{2 R_2 X_{Lp}}{Q_L} \tag{31}$$

$$n = R_2 X_{Lp}\left(-R_1 + X_{cs}\left(\frac{1}{Q_L} - \frac{1}{Q_c}\right)\right) \tag{32}$$

Calculation of XCS and thus CS is also derived in a similar fashion by solving the quadratic equation (15)

$$X_{cp}{}^2(pr - km) + X_{cp}(ps + qr - kn - lm) + (qs - \ln) = 0 \tag{33}$$

Where,

$$p = \left(-R_2 - \frac{X_{Lp}}{Q_L}\right)\left(1 + \frac{1}{Q_L Q_c}\right) + X_{Lp}\left(\frac{1}{Q_L} - \frac{1}{Q_c}\right) \tag{34}$$

$$q = R_2 X_{Lp}\left(\frac{1}{Q_L^2} - 1\right) - \frac{R_2 X_{cs}}{Q_c Q_L} \tag{35}$$

$$r = \left(-R_1 X_{Lp} + \frac{X_{cs} X_{Lp}}{Q_L} + R_2 X_{Lp}\right)\left(1 + \frac{1}{Q_L Q_c}\right) + \frac{R_1 R_2}{Q_c} + R_2 X_{cs}\left(\frac{1}{Q_c^2} - 1\right)$$
$$+ X_{Lp} X_{cs}\left(\frac{1}{Q_L} - \frac{1}{Q_c}\right) \tag{36}$$

$$s = R_2 X_{Lp} \left(X_{cs} - \frac{R1}{Q_L} \right) \tag{37}$$

$$k = (R_2 + \frac{X_{Lp}}{QL}) \; \left(\frac{1}{Qc} - \frac{1}{Q_L} \right) - X_{Lp} \left(1 + \frac{1}{Q_L Q_c} \right) \tag{38}$$

$$l = -\frac{2R_2 X_{Lp}}{QL} \tag{39}$$

$$m = \left(\frac{X_{cs} X_{Lp}}{Qc} + X_{Lp} R_2 \right) \left(\frac{1}{QL} - \frac{1}{Qc} \right) - X_{Lp} R_1 \left(\frac{1}{QL} + \frac{1}{Qc} \right) - R_1 R_2 + \frac{2R_2 X_{cs}}{QL}$$
$$+ X_{cs} X_{Lp} \left(1 + \frac{1}{Q_L Q_c} \right) \tag{40}$$

$$n = R_2 X_{Lp} \left(-R_1 + X_{cs} \left(\frac{1}{QL} - \frac{1}{Qc} \right) \right) \tag{41}$$

The final set components obtained using this Equivalent Impedance method (using (6), (15), (24) and (33)) are listed in Table III. The corresponding S11 plots using these components are shown in Fig. 7 for high to low and low to high matching networks respectively. Therefore the proposed Equivalent Impedance method provides substantial improvement in matching performance both for off-chip and on-chip case. The improvement is more prominent in on-chip case.
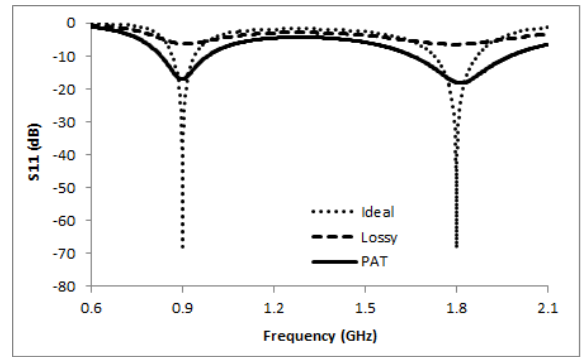
2.2.2 Parasitic Absorption Method

Another method to account the parasitic impact is altering the required source and load impedances depending on the component quality factor (component parasitic). Hence, instead of designing with component parasitic, those (parasitic) are absorbed into source and load impedances. The step by step procedure followed in this method is explained as an algorithm below.

Table IV
Components values for cc-db-bp l-matching network using
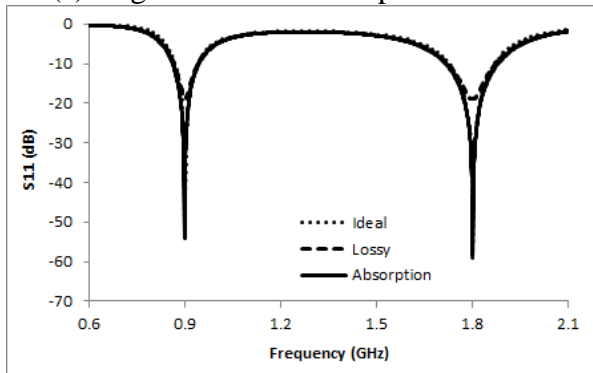Parasitic absorption method.

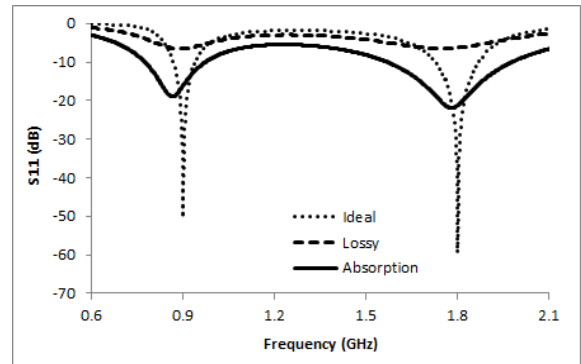| QL, Qc	H to L (500Ω to 50Ω)				L to H (5Ω to 50Ω)			
	Ls (nH)	Cs (pF)	Lp (nH)	Cp (pF)	Ls (nH)	Cs (pF)	Lp (nH)	Cp (pF)
∞, ∞	26.5	0.59	14.8	1.06	2.65	5.89	1.47	10.6
50, 100	24.6	0.63	13.2	1.17	2.62	5.73	1.71	9.11
5, 30	13.3	1.17	8.02	1.94	6.45	2.42	4.53	3.44
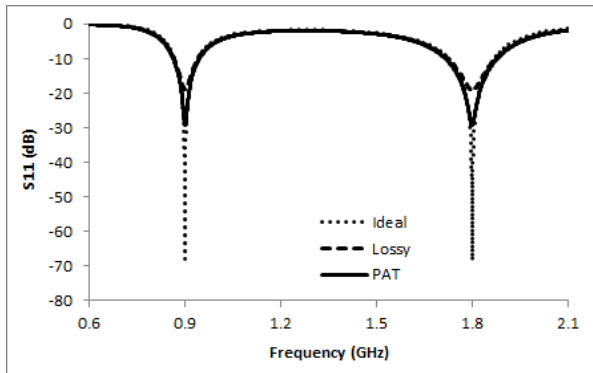
(a) High to Low: Off-Chip

(b) High to Low: On-Chip

(c) Low to High: Off-Chip

(d) Low to High: On-Chip

Fig. 7. S11 response of CC-DB-BP L-matching Networks with derived components
using Parasitic Absorption Method

Table V
Derived component values using equivalent impedance
Method for murata library.

Method	H to L (500Ω to 50Ω)				L to H (5Ω to 50Ω)			
	Ls (nH)	Cs (pF)	Lp (nH)	Cp (pF)	Ls (nH)	Cs (pF)	Lp (nH)	Cp (pF)
Derived	23	0.7	13	1	2.8	5.1	1.7	7
Absorption	23	0.6	13	1.1	3	5.1	1.7	6.8

1) Derive the narrow band L-matching network using ideal method.

2) Convert into CC-DB network using ideal frequency transformation.

3) Compute the equivalent resistance in series and parallel LC sections. The series-parallel conversion is given in (42) and (43);

$$R_p = \frac{Rs^2 + Xs^2}{Rs} \tag{42}$$
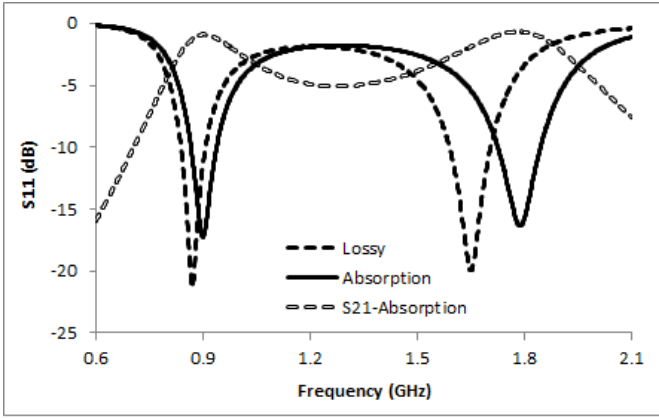
$$X_p = \frac{Rs^2 + Xs^2}{Xs} \tag{43}$$

4) Add equivalent resistance into source or load (which is nearby). This parasitic resistance is absorbed in to load and source.
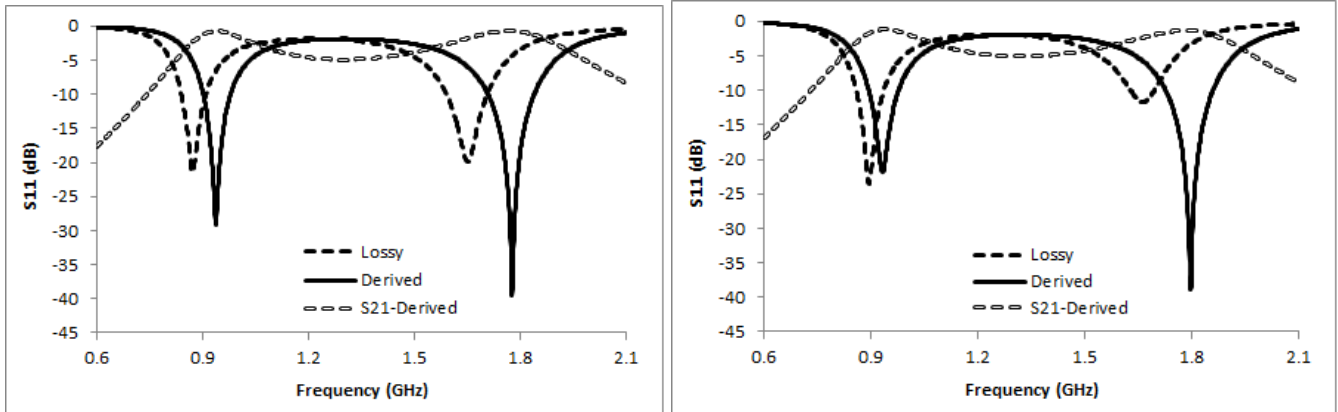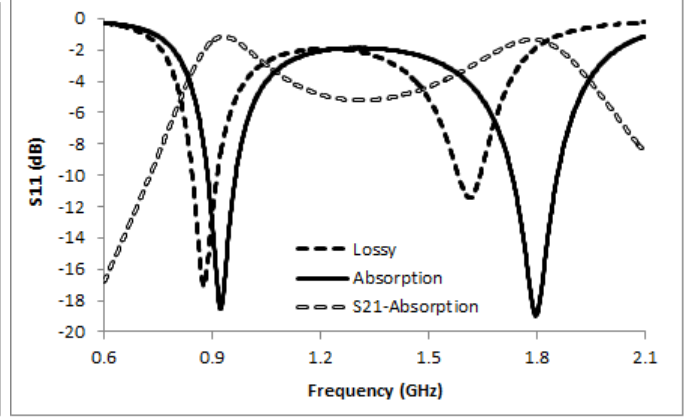

(a) High to Low: Off-Chip   (b)   High to Low: On-Chip

Fig. 9. S11 and S21 response of CC-DB-BP L-matching Network using Murata Components derived by Equivalent Impedance method

17

(c) Low to High: Off-Chip   (d) Low to High: On-Chip

Fig. 10. S11 and S21 response of CC-DB-BP L-matching Network using
Murata Components designed by Absorption method

$$R_{2new} = \frac{1}{\dfrac{1}{R_{Lp}} + \dfrac{1}{R_{cp}} + \dfrac{1}{R_2}} \tag{44}$$

$$R_{1new} = R_{Ls} + R_{cs} + R_1 \tag{45}$$

5) Derive again all components for the new source and load impedance using parasitic aware method given in the above subsection III-B.

The obtained component values for CC-DB-BP L-matching circuit to match from 500 to 50 and 5 to 50 are given in Table IV. The corresponding S11 plots are shown in Fig. 8 and 9. The result shows that the matching is improved from the lossy components circuit and frequency drifting also almost null even with low-Q case. Further, the proposed methods are validated using real components in the following subsection.

2.2.3. Validation with Real Components

The proposed impedance matching methods are validated using practical components from UMC 0.18um RF CMOS process (on chip) and Coilcraft and Murata (off chip) libraries. The simulations are done using Cadence Spectre-RF

(onchip) and Agilent ADS (off-chip) simulation tools respectively.Coilcraft inductors of CCI 0402CS series which has a quality factor around 53 and GJM15 series of capacitors from Murata libraries are used. Onchip spiral inductors (Q=5) and MIM capacitors from UMC 0.18um RF CMOS process are used for onchip validation.

The matching performance and insertion loss are plotted and verified in terms of input reflection (S11) and forward gain (S21). Obtained values for dual band matching using off-chip (Coilcraft and Murata) components are listed in Table V. The corresponding performances of off-chip networks are shown in Fig. 10 and 11. Derived component values for on-chip (UMC 0.18um RF CMOS) matching are listed in Table VI

Table VI

Derived component values using equivalent impedance

Method for umc 0.18um library.

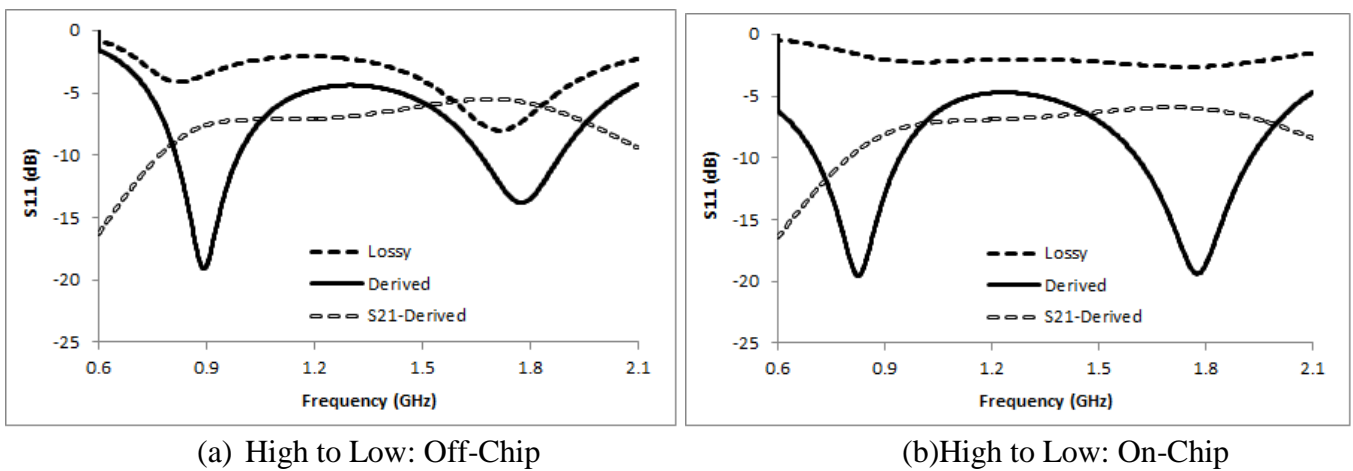| Method	H to L (500Ω to 50Ω)				L to H (5Ω to 50Ω)			
	Ls (nH)	Cs (pF)	Lp (nH)	Cp (pF)	Ls (nH)	Cs (pF)	Lp (nH)	Cp (pF)
Derived	10.7	1.44	6.52	2.39	5.51	2.83	3.86	4.04
Absorption	13.2	1.17	8.02	1.94	5.46	2.85	3.78	4.13

(a) High to Low: Off-Chip   (b)High to Low: On-Chip

Fig. 11. S11 and S21 response of CC-DB-BP L-matching Network using

UMC 0.18um Components derived by Equivalent Impedance method

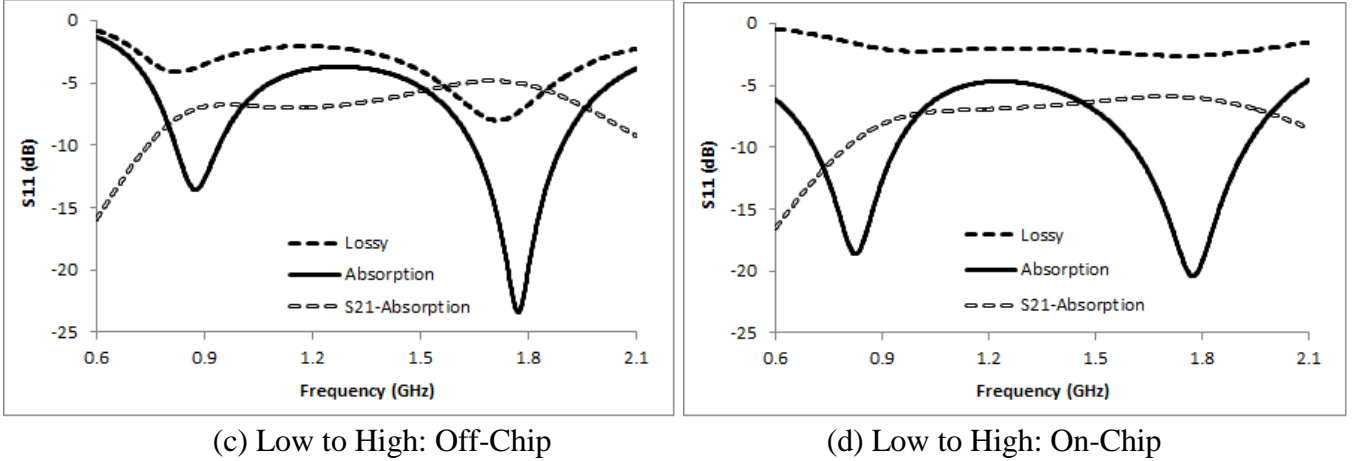(c) Low to High: Off-Chip   (d) Low to High: On-Chip

Fig. 12. S11 and S21 response of CC-DB-BP L-matching Network using
UMC 0.18um Components designed by Absorption method

and its corresponding performance plots are given in Fig. 12, 13 respectively. From the result plots (Fig. 10 and 11) it is observed that the shift in frequency due to inherent parasitics of the real offchip components was considerable and this impact is almost eliminated by the proposed method. In on-chip scenario the matching performance has greatly improved. On the other hand, the insertion loss is more in on-chip implementation (Fig. 12 and 13). This is probably because of on-chip inductors have higher internal resistance which make the loss and is unavoidable. Further in the next section, the proposed method is applied for designing quad band L-matching network.

2.3. Parasitic Aware Quad-Band Matching

The design methods proposed in the above section are extended to design concurrent quad band L-matching network including the component parasitics. A typical concurrent quad band L-matching network which is shown in Fig. 14 is taken as example circuit for the design explanation.

The transformation between frequencies and the ideal circuit design procedures are taken as given in [13]. GSM900, DCS1800, ISM2400 and WiFi-5GHz bands are considered for this design. The proposed Equivalent Impedance and

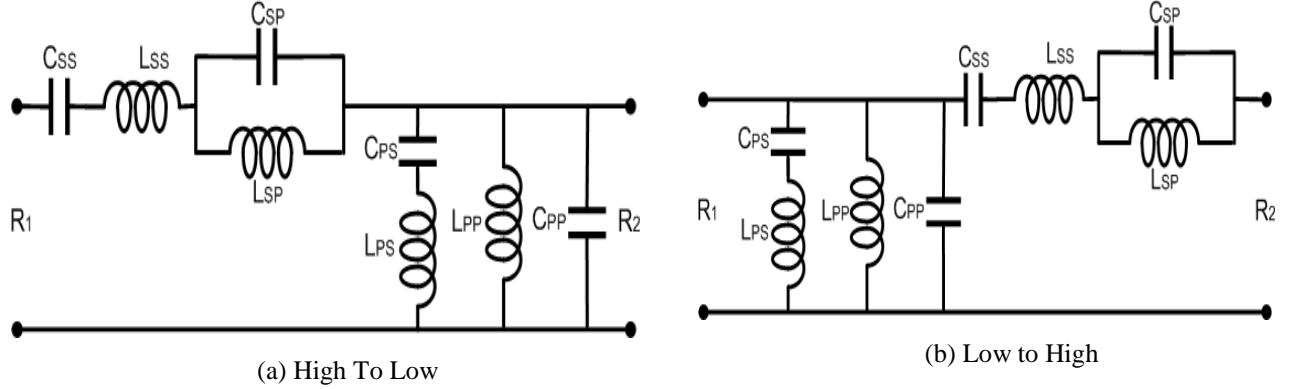Parasitic Absorption methods for designing concurrent quad band L-matching network design is explained below.

(a) High To Low

(b) Low to High

Fig. 13. Concurrent Quad Band L-matching Network

2.3.1 Equivalent Impedance Method for Quad Band Network

Initial steps in this design method are followed same as explained in Section III-B. Further the transformation is done to another frequency as well. The step by step procedure is given below as algorithm.

1) Derive the narrow band L-matching network using PAT L-matching method for the frequency below.

$$wm = w_1 - w_2 + w_3 - w_4 \tag{46}$$

2) Convert this into concurrent dual band circuit using the method given in Section III-B for the frequency below.

$$w_{r1} = \sqrt{(w_3 - w_2)(w_4 - w_1)} \tag{47}$$

3) Do the back calculation for finding more accurate component values.

4) Compute the quad band network components by ideal method for the below frequency.

$$w_{r2} = \sqrt{w_2 w_3} \tag{48}$$

Table VII
Components values for quad-band network using equivalent impedance method at 450MHz, 900MHz, 1.2GHz and 2.4GHz.

QL, Qc	500Ω to 50Ω			5Ω to 50Ω		
	∞, ∞	50, 100	5, 30	∞, ∞	50, 100	5, 30
Lss (nH)	14.4	12.5	5.71	1.44	1.56	2.03
Css (pF)	1.62	1.86	4.10	16.2	14.9	11.5
Lsp (nH)	7.83	6.81	3.09	0.78	0.85	1.09
Csp (pF)	2.99	3.32	7.58	29.9	27.5	21.3
Lps (nH)	74.7	65.5	30.0	7.48	7.79	10.9
Cps (pF)	0.31	0.35	0.78	3.13	3.0	2.15
Lpp (nH)	40.0	35.5	16.2	4.05	4.22	5.90
Cpp (pF)	0.57	0.66	1.44	5.78	5.55	3.97

The derived component values for different frequency sets and quality factors are listed in Table VII and VIII. The corresponding matching performances are plotted in terms of (S11) and shown in Fig.15- 18.

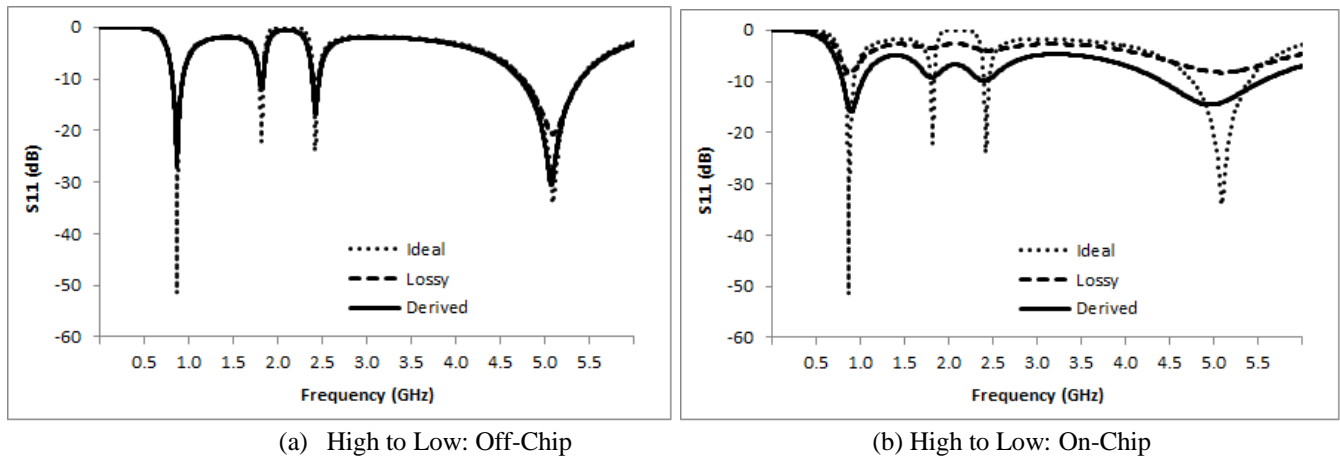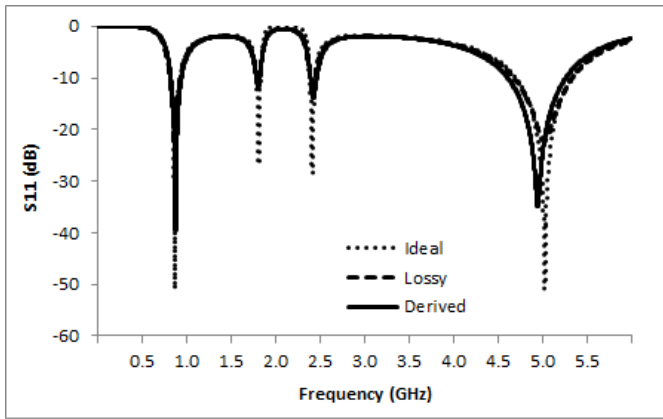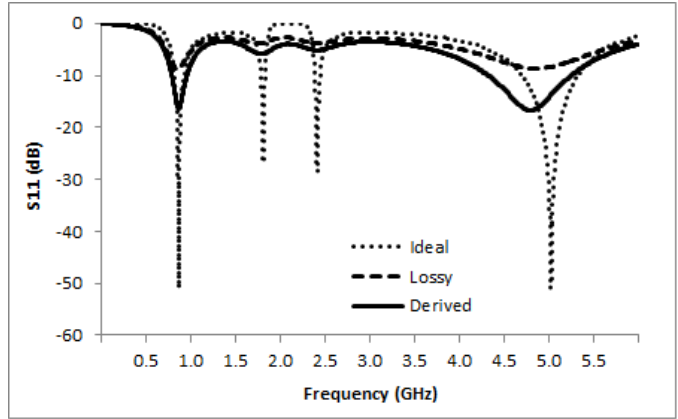(a) High to Low: Off-Chip   (b) High to Low: On-Chip

Fig. 16. S11 response of CC-QB HtoL L-matching Network with derived components using Equivalent Impedance method at 900MHz, 1.8GHz, 2.4GHz and 5GHz
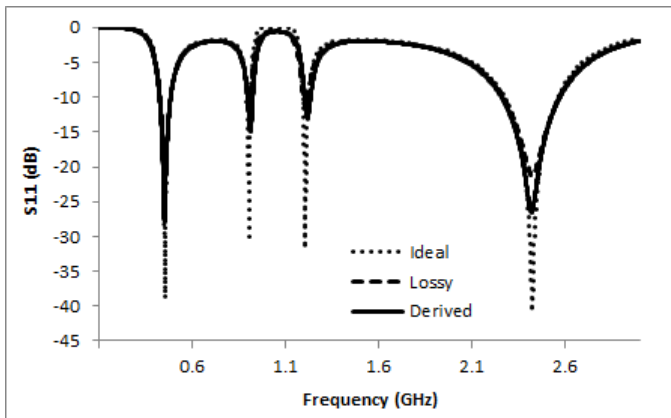
(c) Low to High: Off-Chip   (d) Low to High: On-Chip

Fig. 17. S11 response of CC-QB LtoH L-matching Network with derived components using Equivalent Impedance method at 900MHz, 1.8GHz, 2.4GHz and 5GHz
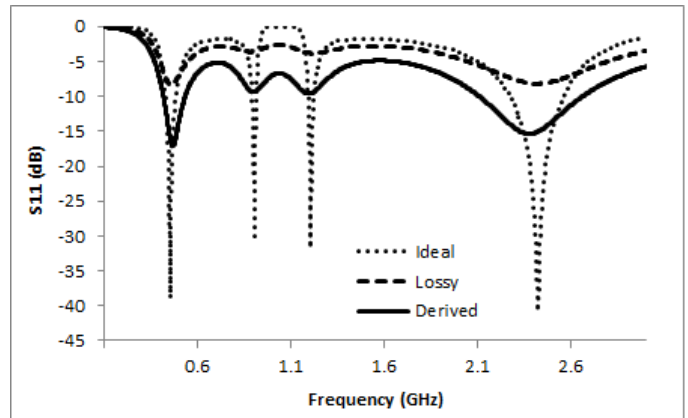
Table VII
Components values for quad-band network using equivalent impedance method at 450MHz, 900MHz, 1.2GHz and 2.4GHz.

	500Ω to 50Ω			5Ω to 50Ω		
QL, Qc	∞, ∞	50, 100	5, 30	∞, ∞	50, 100	5, 30
Lss (nH)	6.7	5.86	2.66	0.67	074	1.01
Css (pF)	0.86	0.99	2.2	8.69	7.86	5.84
Lsp (nH)	3.87	3.37	1.53	0.38	0.42	0.56
Csp (pF)	1.51	1.73	3.82	15.1	13.6	10.4
Lps (nH)	37.7	33.1	15.1	3.78	3.94	5.52
Cps (pF)	0.15	0.17	0.38	1.55	1.48	1.02
Lpp (nH)	21.7	19.0	8.73	2.17	2.27	3.02
Cpp (pF)	0.26	0.30	0.67	2.69	2.58	1.89

(b) High to Low: Off-Chip   (b) High to Low: On-Chip

23

Fig. 14. S11 response of CC-QB HtoL L-matching Network with derived components using Equivalent Impedance method at 450MHz, 900MHz, 1.2GHz and 2.4GHz

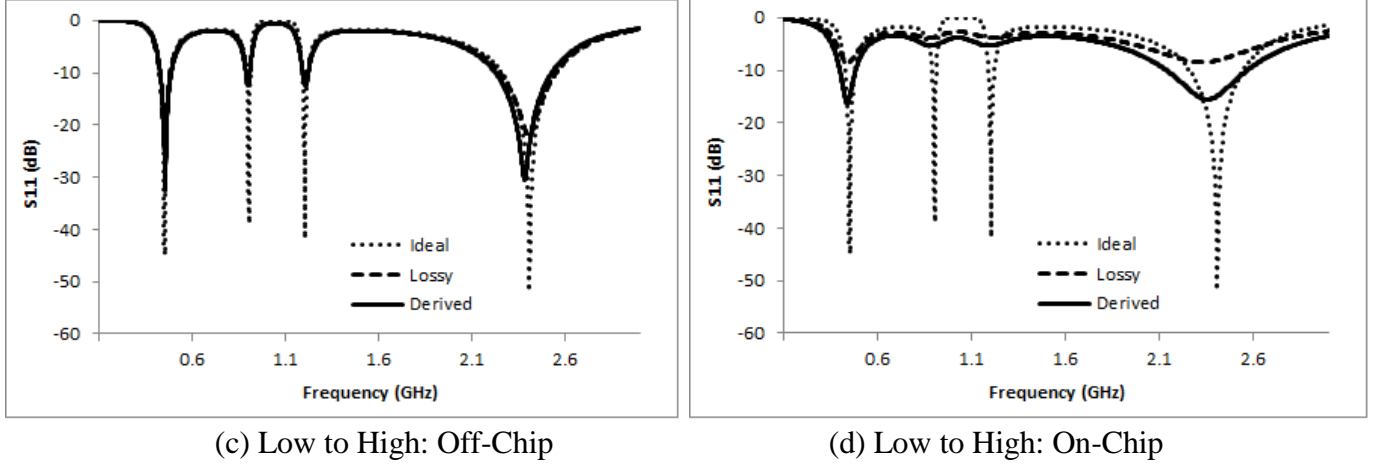(c) Low to High: Off-Chip   (d) Low to High: On-Chip

Fig. 15. S11 response of CC-QB LtoH L-matching Network with derived components using Equivalent Impedance method at 450MHz, 900MHz, 1.2GHz and 2.4GHz

2.3.2. Parasitic Absorption Method for Quad Band Network

Initial steps in this design method are followed same as explained in Section III-C till the dual band extension. Further the quad band is done by another frequency transformation. The step by step procedure is given below as an algorithm.

1) Derive the narrow band L-matching network using ideal method for the frequency.

$$wm = w_1 - w_2 + w_3 - w_4 \qquad (49)$$

2) Convert into concurrent dual band network using ideal frequency transformation for the frequency.

$$w_{r1} = \sqrt{(w_3 - w_2)(w_4 - w_1)} \qquad (50)$$

3) Convert into concurrent quad band network using ideal frequency transformation for the frequency.

$$w_{r2} = \sqrt{w_2 w_3} \qquad (51)$$

4) Compute the equivalent resistance in all series and parallel LC sections using (42) and (43) and transform into convenient form.

24

5) Add equivalent resistance into source or load (which is nearby). This parasitic resistance is absorbed in to load and source.

$$R_{2new} = \cfrac{1}{\cfrac{1}{R_{Lps} + R_{cps}} + \cfrac{1}{R_{Lpp}} + \cfrac{1}{R_{cpp}} + \cfrac{1}{R_2}} \tag{53}$$

$$R_{1new} = R_{Lss} + R_{css} + \cfrac{1}{\cfrac{1}{R_{Lsp}} + \cfrac{1}{R_{csp}}} + R_1 \tag{54}$$

Table VIII

Components values for quad-band network using Parasitic Absorption method at 900MHz, 1.8GHz, 2.4GHz and 5GHz.

	500Ω to 50Ω			5Ω to 50Ω		
QL, Qc	∞, ∞	50, 100	5, 30	∞, ∞	50, 100	5, 30
Lss (nH)	6.7	5.86	2.66	0.67	074	1.01
Css (pF)	0.86	0.99	2.2	8.69	7.86	5.84
Lsp (nH)	3.87	3.37	1.53	0.38	0.42	0.56
Csp (pF)	1.51	1.73	3.82	15.1	13.6	10.4
Lps (nH)	37.7	33.1	15.1	3.78	3.94	5.52
Cps (pF)	0.15	0.17	0.38	1.55	1.48	1.02
Lpp (nH)	21.7	19.0	8.73	2.17	2.27	3.02
Cpp (pF)	0.26	0.30	0.67	2.69	2.58	1.89

6) Derive again all components for the new source and load impedance using parasitic aware method given in the above subsection III-B for !m and !r1.

7) Finally make an ideal dual to quad band transformation for wr2. Obtained components for high to low and low to high matching using the quad band absorption method are listed in Table IX and X. The corresponding S11 profiles are shown in Fig. 19 - 22 respectively.

2.3.3 Validation with Practical Components

The practical implementation of the proposed method for quad band matching is done in the same way as in dual band. The practical components (same as dual band) from UMC 0.18um RF CMOS process (on chip) and Coilcraft and Murata (off chip) libraries are used here as well. Frequency range is a crucial issue in this implementation. The quality factor of offchip capacitors are more frequency dependent due to the complexity of its internal parasitics (equivalent circuit) [?]. Due to this, when the desired bands are widely separated the matching will be imperfect. On the other hand, self resonance frequency (FSR) of high value on-chip inductors are considerably low. This limits their usage in lower frequencies. Hence, designing for same frequencies in both on-chip and off-chip scenario with practical components available in present day will be a difficult task. Though it is a trade off in frequency selection ISM450, GSM900, GPS1200 and ISM2400 frequency bands are chosen for validation which will give better performance in off-chip scenario.

The obtained components for off-chip and on-chip categories are listed in Table XI. The corresponding S11 and S21 plots for the same are shown in Fig. 23 and 24. The results show that the proposed method is giving better performance in off-chip scenario. In on-chip case, the matching improvement is less and in selective frequencies. This kind of response may be due to lower self resonance frequencies of high value inductors. This issue can be taken in future for further improvement.

TABLE XI
COMPONENTS VALUES FOR QUAD-BAND NETWORK USING COILCRAFT,
MURATA AND UMC 0.18UM LIBRARIES

Method	Equivalent	Absorption	Equivalent	Absoption
Lss (nH)	12.0	12.0	2.03	1.9
Css (pF)	1.80	1.8	11.5	11.2
Lsp (nH)	6.8	6.8	1.10	1.08
Csp (pF)	3.0	3.3	21.3	21.7
Lps (nH)	68.0	68.0	10.9	11.0
Cps (pF)	0.3	0.3	2.15	2.09
Lpp (nH)	36.0	36.0	5.89	6.0
Cpp (pF)	0.5	0.5	3.97	3.85

(a) Equivalent   (b) Absorption
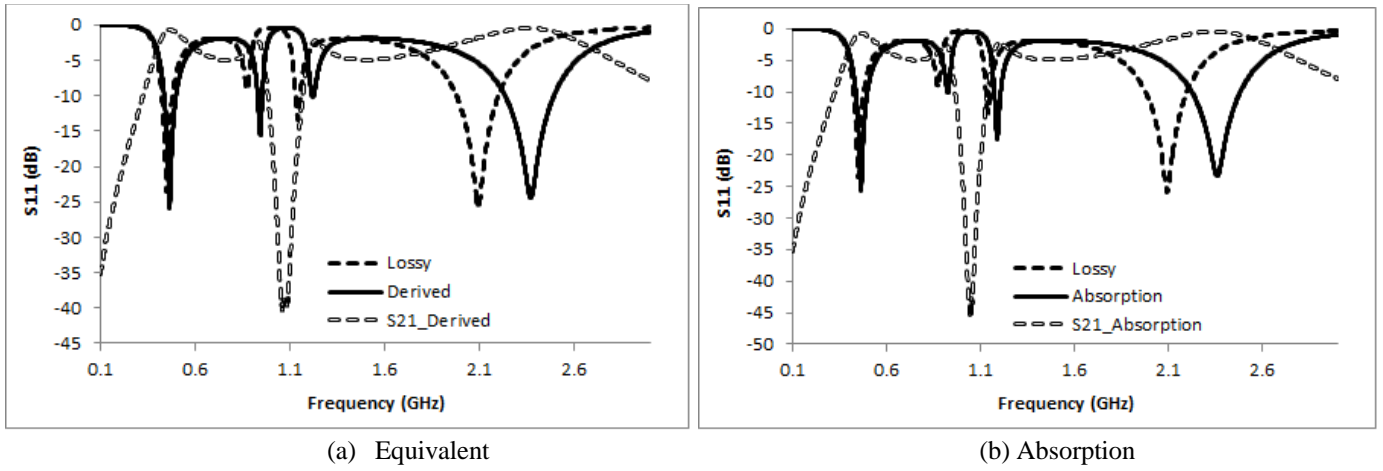
Fig. 22. S11 and S21 response of CC-QB-BP L-matching Network using Coilcraft, Murata Components

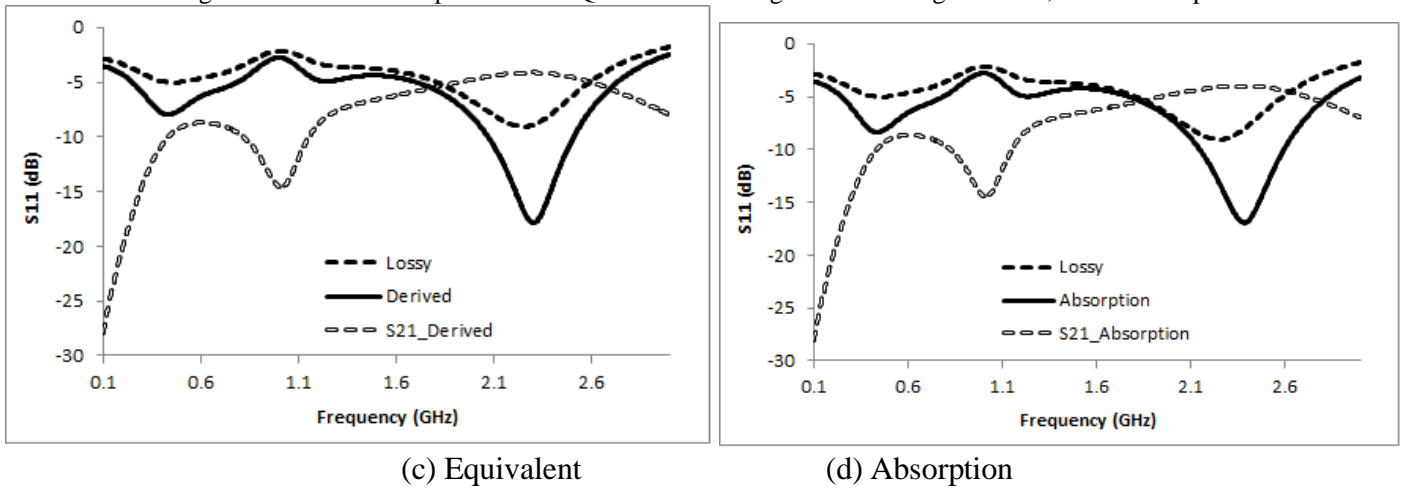(c) Equivalent   (d) Absorption

Fig. 23. S11 and S21 response of CC-QB-BP L-matching Network using UMC 0.18um Components designed

2.4 Conclusion

The proposed two methods, Equivalent Impedance method and Parasitic Absorption method, for designing concurrent multi-band L-matching networks including the component non-idealities. Both methods show better performance in terms of matching quality and frequency even with low quality factor components.

3 Broadband impedance matching

3.1 Introduction

 In broadband RF circuits, the matching has to be achieved over a band of frequencies. There are different approaches proposed for broadband matching. One among is using LC-sections (Lowpass and Highpass). LC-sections are cascaded to obtain broader bandwidth. With cascaded sections, the lowest Q (and widest bandwidth) is achieved when the intermediate impedance is the geometric mean of the source and load impedances.

3.2 Broadband matching design using Filter Design Approach

The filter synthesis approach to broadband impedance matching network design usually involves mapping, a frequency domain transformation to the desired pass band. Perhaps the most well known frequency transformation is the Lowpass to Bandpass.

$$s = QT \left(\frac{w0}{p} + \frac{p}{w0} \right) \tag{55}$$

Where, $QT = \frac{\sqrt{f1 f2}}{f2 - f1}$ f1, f2 are corner frequencies.

$$Ls = rLs$$
$$Cs = \frac{1}{wc^2 Ls}$$
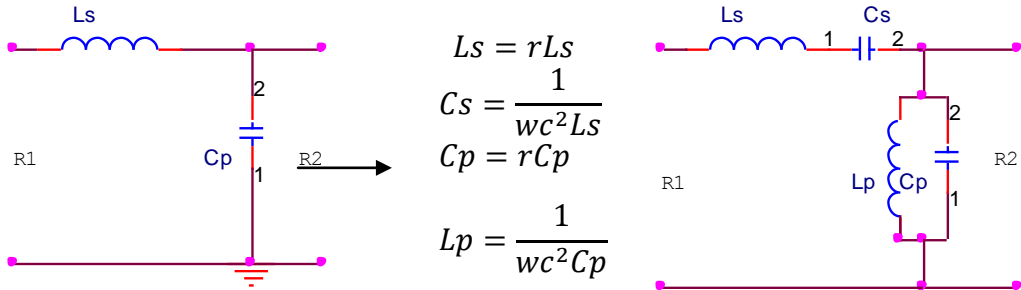$$Cp = rCp$$
$$Lp = \frac{1}{wc^2 Cp}$$

Fig 3.1: Transformation from Lowpass LC-section to Bandpass network

The feature of mapping is that it allows network conversions on an element-by-element impedance basis. Consider an inductor of Lowpass complex impedance SL. Two impedance terms results when equation () is applied:

$$\frac{QTw0L}{p} + \frac{QTL}{w0}p \qquad (56)$$

The first term appears to be capacitor and second term behaves as an inductor.

Hence, a series LC branch results from a Lowpass inductor. Similarly, a capacitor of Lowpass map into parallel LC branch.

In Figure 2, ωc is the center frequency of the target frequency range defined as

$$wL + \frac{(wH - wL)}{2} = wL + \frac{Bw}{2} \qquad (57)$$

BW is the bandwidth required for the target circuit. Note that ωH and ωL are the upper and lower stop frequencies respectively. Parameter *r* is defined by $\omega c/BW$. Since we are interested in signal reflection and not the 3dB bandwidth, the center frequency is chosen as ωc, unlike the general bandpass filter development procedure [5], which defines

$$wc = \sqrt{wHwL} \qquad (58)$$

The bandpass filter synthesized with the center frequency ωc has minimum power reflection at the center frequency so that it satisfies the impedance match over the entire target bandwidth at the cost of small gain reduction in the upper frequency range.

The design of broadband matching is detailed by an example.

Design broadband impedance matching from 50Ω to 20Ω with fL=600MHz and fU=2.6GHz.

Step 1: Design Lowpass network from parasitic aware technique at

$$fm = f2 - f1 \qquad (59)$$

Broadband design technique must consider the entire frequency band in the design procedure. It is usually sufficient to work with the center and end frequencies.

Step2: Transform Lowpass to bandpass by replacing inductor with series LC branch and capacitor by shunt LC branch.

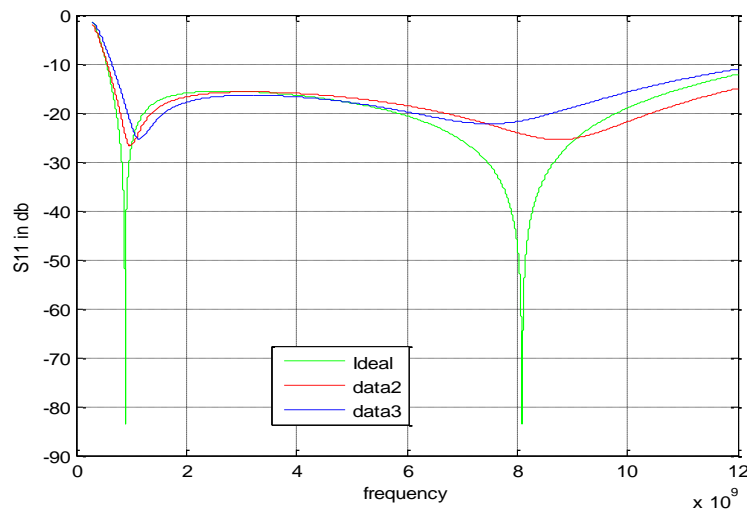Step 3: Obtain the transformed components from impedance equivalent method at

$$fc = fL + \frac{Bw}{2} \qquad (60)$$

Fig 3.2: s11 plot for High to Low bandpass network for R1=50, R2=20

3.3 Transformation of LC-section to Bandpass network

Cascaded LC-section with source impedance R1 and load impedance R2 is transformed to bandpass by replacing inductor with series LC branch and capacitor with shunt LC as shown in fig 17.
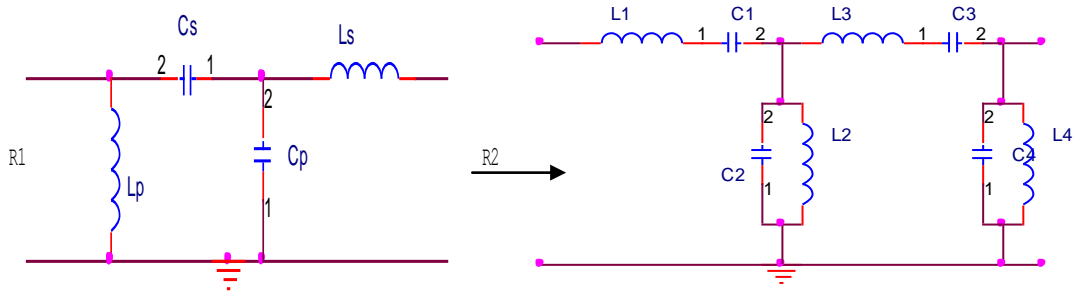
Fig 3.3: Cascaded Highpass with Lowpass transformed to bandpass

The component values are tabulated in table. The parasitic aware technique as been used to obtain LC values.

	L1	C1	L2	C2	L3	C3	L4	C4
Ideal	3.21	9.72	30.9	1.01	4.06	7.69	38.9	0.83
QL=5,Qc=30	3.48	8.97	24.7	1.26	4.40	7.10	31.3	0.99
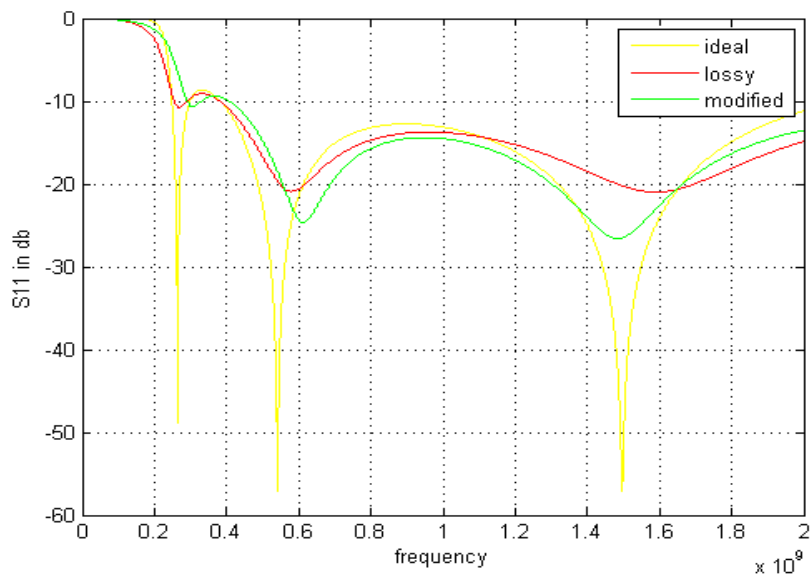
Fig 3.4: S11 plot for transformed Bandpass network

3.4 Proposed Band Stretching method

In band stretching technique the cascaded LC section are designed for different cutoff frequencies. The Lowpass LC section are designed at higher cutoff frequency fH and the highpass LC section with low cutoff frequency fL

Procedure:

Step 1: consider the minimum input reflection coefficient over the band,

For example,   S11 < -10dB

Step2:   Calculate load impedance ZL=ZL$_{real}$+j ZL$_{img}$ from given minimum S11

$$ZL(max) \geq Zs \; \frac{1 + S11}{1 - S11} \tag{61}$$

Where , Zs=50 ohm

The component reactance are given in equation (62) and (63). Where wH and wL are the Higher and Lower cutoff frequency respectively.

Step3:

$$Xcs = \frac{1}{wL \; Cs} \qquad\qquad XLp = wL \; Lp \tag{62}$$

$$Xcp = \frac{1}{wH \; Cp} \qquad\qquad XLs = wL \; Ls \tag{63}$$

wH and wL for maximum band stretching so that the band should not be above the given S11= -10dB

Step4:   ZL$_{img}$= f(wH, wL)

ZL$_{real}$= f(wH, wL)

From above equation we can get wH and wL. Calculate Lp,Cs, Ls,Cp from wH and wL

The reflection coefficient   S11 is given by
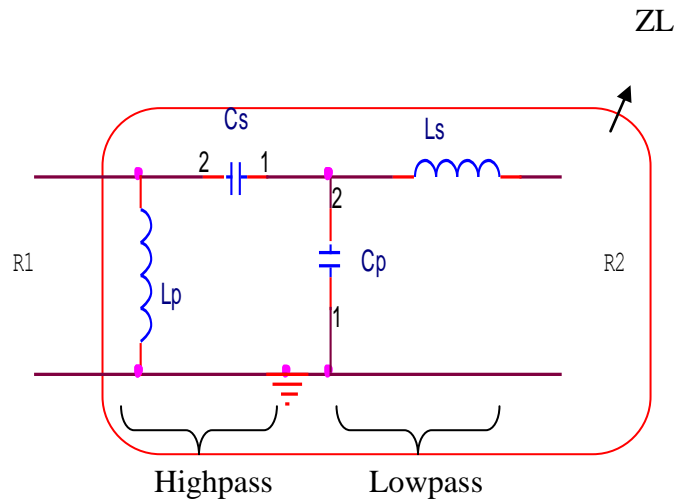
$$S11 = \frac{ZL - Zs}{ZL + Zs} \tag{64}$$

The input reflection coefficient should be less than $S11(min)$.

$$S11(min) \leq \frac{ZL - Zs}{ZL + Zs} \tag{65}$$

The load impedance for S11(min) is given by

$$ZL(max) \geq Zs \, \frac{1 + S11}{1 - S11} \tag{66}$$

The load impedance is in the form of ZL=ZLreal + j ZLimg

Zreal and Zimg equation for cascaded Highpass and Lowpass network is given as

ZL_{img}

$$\geq - \frac{xLp(-R2^2(xcp + xcs)(xcp + xcs - xLp) - (xcpxcs - (xcp + xcs)xLs)(xcp(xcs - xLp) - (xcp + xcs - xLp)xLs))}{R2^2(xcp + xcs - xLp)^2 + (xcp(xcs - xLp) - (xcp + xcs - xLp)xLs)^2} \tag{67}$$

$$ZL_{real}$$

$$\geq \frac{R2xcp^2xLp^2}{R2^2(xcp + xcs - xLp)^2 + (xcp(xcs - xLp) - (xcp + xcs - xLp)xLs)^2} \tag{68}$$

Since we know the ZL real and ZL img for given S11(min), higher cutoff frequency fH and lower cutoff frequency fL can be calculated for a given centre frequency.
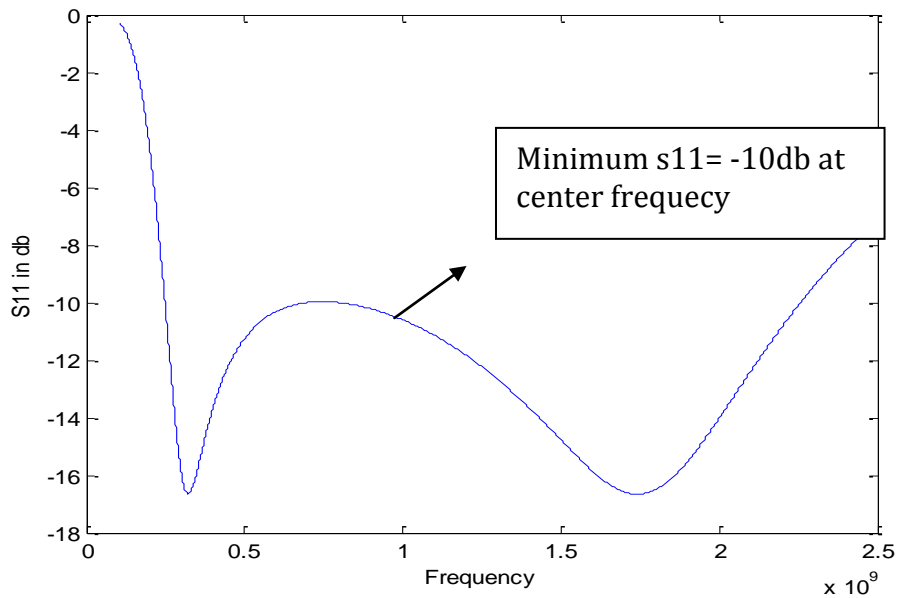

Fig 3.5: S11 plot for cascaded Highpass and Lowpass network

For given example S11(min) = -10dB , Zs=50Ω , the S11 plot is shown in fig. 3.5. the center frequency is 900MHz, the calculated fL and fH are 650MHz and 1.7GHz. The entire band is below the given S11

3.5 Conclusion

The LC Ladder network are designed using Band stretching technique for given input reflection coefficient. Uniformity over a band can be obtained from this technique.

4 Parasitic impact on Broadband impedance matching

4.1 Introduction

In narrow band matching the impact of parasitic are significant. Component parasitic degrades the matching performance. To improve the matching performance different generic design approaches are proposed [1]. The impact of these components parasitic is detailed by considering Lowpass L-section. Consider the Lowpass L-section
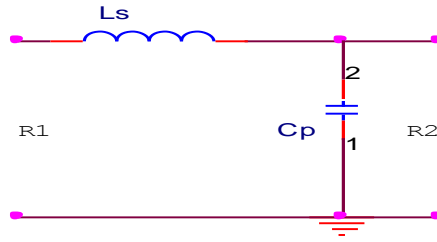

Fig 4.1: Lowpass L-section

The real impedance of Lowpass L-network is given by,

$$Z_{real} = \frac{Q_L X_{cp}^2 (Q_L R_2 + X_{Ls})}{Q_L^2 (R_2^2 + (X_{cp} - X_{Ls})^2) + 2 Q_L R_2 X_{Ls} + X_{Ls}^2} \qquad (69)$$

The imaginary impedance,

$$Z_{imag} = \frac{X_{cp}(X_{cp} - X_{Ls})X_{Ls} - X_{cp}\left(R_2 + \frac{X_{Ls}}{Q_L}\right)^2}{(X_{cp} - X_{Ls})^2 + \left(R_2 + \frac{X_{Ls}}{Q_L}\right)^2} \qquad (70)$$

In real impedance equation, the observation is that, the Quality factor of inductor is present in almost all terms which is the cause for degradation in reflection

35

coefficient for real components shown in s11 plot fig. The slight frequency shift in practical case is because of QL in imaginary impedance.
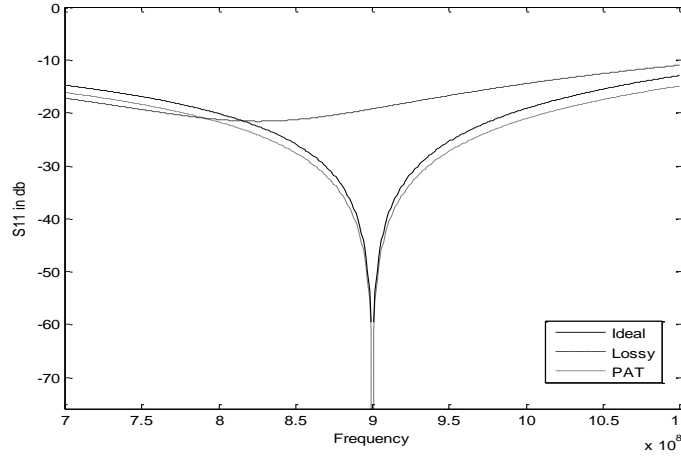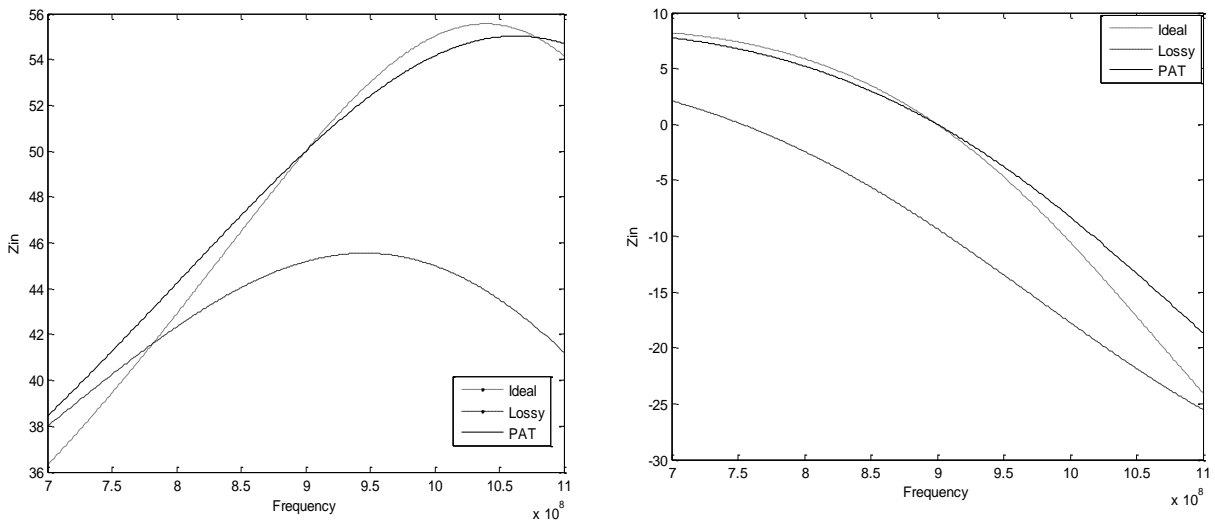

Fig 4.2: s11 plot of Lowpass L-section for on-chip case(QL=5)

Real impedance

Imaginary impedance

Fig 4.3: Impedance plot of Lowpass L-section for on-chip case(QL=5)

The matching performance in narrowband degrades in real environment. It can be in seen in reflection coefficient plot S11. The observation is that the impact of component parasitic in narrowband matching is more.

Broadband matching can be achieved from LC ladder approach and by Filter design approach. Further will discuss the impact of component parasitic on broadband impedance matching performance.

4.2 Cascade of LC-sections

Cascading LC-sections can lead to Low Q in turn increases the bandwidth. The unloaded quality factor is inversely proportional to bandwidth. Peaky response will achieve from high Q.

$$Q = \frac{f0}{BW} \tag{71}$$

4.2.1 Cascade of two LC-section

Let us consider the Cascade of Highpass to Lowpass LC-section with a lossy inductor whose losses are modeled as a small series resistance $\square_\square$. Usually the inductor losses are specified in terms of quality factor (QL). The relation between r and QL is given as $r_L = \frac{X_L}{Q_L}$.
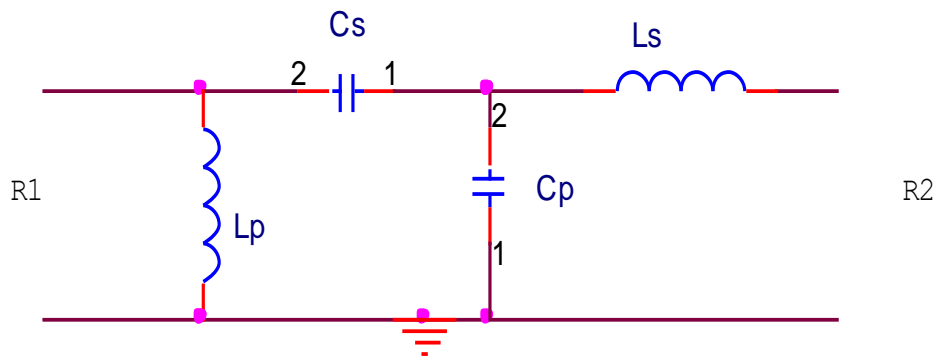

Fig 4.4: Highpass network is cascaded with Lowpass network

In Highpass L-network the source impedance R1 is matched to intermediate impedance Ri, which is the geometric mean of R1 and load impedance R2. This intermediate impedance is matched to load by Lowpass network. The intermediate resistance,

$$Ri = \sqrt{R1R2} \tag{72}$$

$$Q = \sqrt{\frac{R1}{Ri} - 1} + \sqrt{\frac{Ri}{R2} - 1} \tag{73}$$

Both capacitor and inductor are lossy, in general the inductor loss dominate the overall loss in a matching network. In this section we analyze the effect of inductor with finite quality factor on the reflection coefficient of the broadband matching network.

The real impedance is given by,

Z_{real}

$$= \frac{\begin{aligned}&X_{Lp}(X_{cp}^2 X_{cs}^2 + R_2^2(X_{cp} + X_{cs})^2 + \frac{(1+Q_L^2)}{Q_L}R_2 X_{cp}^2 X_{Lp} + \\ &\left(2(X_{cp} + X_{cs})\left(-X_{cp}Xcs + \frac{R_2}{QL}(X_{cp} + X_{cs})\right) + \frac{(1+Q_L^2)}{Q_L^2}X_{cp}^2 X_{Lp}\right)XLs + \frac{(1+Q_L^2)}{Q_L^2}(X_{cp} + X_{cs})^2 X_{Ls}^2)\end{aligned}}{\begin{aligned}&\left(Q_L R_2(X_{cp} + X_{cs} - X_{Lp}) + X_{cp}X_{Lp} + (X_{cp} + X_{cs} - 2X_{Lp})X_{Ls}\right)^2 \\ &+ \left(\frac{R_2 X_{Lp}}{Q_L} + \frac{X_{Lp}X_{Ls}}{Q_L^2} + (X_{cs} - X_{Lp})X_{Ls} + X_{cp}(-X_{cs} + X_{Lp} + X_{Ls})\right)^2\end{aligned}} \tag{74}$$

In real impedance equation $\frac{(1+Q_L^2)}{Q_L^2}$ can be approximated to 1 since $Q_L^2 \gg 1$. The terms which are multiplied or divided by Q_L are of 10^{-3} range, hence the impact of Q_L is less.

The simplified expression after equating $\frac{(1+Q_L^2)}{Q_L^2} = 1$ and neglect Q_L which the multiplier or divider of small value is given as,

Z_{real}

$$= \frac{\begin{aligned}X_{Lp}(X_{cp}^2 X_{cs}^2 + R_2^2(X_{cp} + X_{cs})^2 + Q_L R_2 X_{cp}^2 X_{Lp} + \\ \left(2(X_{cp} + X_{cs})\left(-X_{cp}Xcs + \frac{R_2}{Q_L}(X_{cp} + X_{cs})\right) + X_{cp}^2 X_{Lp}\right)XLs + (X_{cp} + X_{cs})^2 X_{Ls}^2\end{aligned}}{\begin{aligned}\frac{1}{Q_L}((Q_L R_2(X_{cp} + X_{cs} - X_{Lp}) + X_{cp}X_{Lp} + (X_{cp} + X_{cs} - 2X_{Lp})X_{Ls})^2 \\ + \left(R_2 X_{Lp} + X_{Lp}X_{Ls} + Q_L\left((X_{cs} - X_{Lp})X_{Ls} + X_{cp}(-X_{cs} + X_{Lp} + X_{Ls})\right)\right)^2)\end{aligned}} \quad (75)$$

For example, a broadband matching network with source impedance of 50Ω and load impedance of 20Ω, the real impedance for ideal values at desired frequency is,

$$Z_{real} = \frac{QL(59.7358 + QL(107.5534 + QL(75.8565 + 49.9165QL)))}{0.33191 + QL(0.8749 + QL(2.7383 + QL(1.5219 + 1.QL)))} \quad (76)$$

$$Z_{real} = \frac{\frac{59.7358}{QL^3} + \frac{107.5534}{QL^2} + \frac{75.8565}{QL} + 49.9165}{\frac{0.33191}{QL^4} + \frac{0.8749}{QL^3} + \frac{2.7383}{QL^2} + \frac{1.5219}{QL} + 1} \quad (77)$$

As Q increases the first and second terms in the numerator and first, second and third terms in the denominator will give negligible values hence can be neglected. The expression becomes,

$$Z_{real} = \frac{\frac{75.8565}{QL} + 49.9165}{\frac{1.5219}{QL} + 1}$$

The simplified expression of real impedance equation,

$$Z_{real} = \frac{\begin{aligned}X_{Lp}(X_{cp}^2 X_{cs}^2 + R_2^2(X_{cp} + X_{cs})^2 + \\ \frac{(2(X_{cp} + X_{cs})(-X_{cp}Xcs) + X_{cp}^2 X_{Lp})XLs + (X_{cp} + X_{cs})^2 X_{Ls}^2)}{Q_L} + R_2 X_{cp}^2 X_{Lp}^2\end{aligned}}{\begin{aligned}\frac{2R2\left(X_{cp}^2 X_{Lp} + (X_{cp} + X_{cs} - X_{Lp})^2 X_{Ls}\right)}{Q_L} + \\ \left(R2^2(X_{cp} + X_{cs} - X_{Lp})^2 + \left((X_{cs} - X_{Lp})X_{Ls} + X_{cp}(-X_{cs} + X_{Lp} + X_{Ls})\right)^2\right)\end{aligned}} \quad (78)$$

The above equation can be rewritten as

$$
Z_{real}
$$

$$
= \frac{\frac{X_{Lp}(X_{cp}^2 X_{cs}^2 + R_2^2(X_{cp}+X_{cs})^2 + (2(X_{cp}+X_{cs})(-X_{cp}Xcs) + X_{cp}^2 X_{Lp})XLs + (X_{cp}+X_{cs})^2 X_{Ls}^2)}{Q_L(R2^2(X_{cp}+X_{cs}-X_{Lp})^2 + ((X_{cs}-X_{Lp})X_{Ls} + X_{cp}(-X_{cs}+X_{Lp}+X_{Ls}))^2)} + \frac{R_2 X_{cp}^2 X_{Lp}^2}{(R2^2(X_{cp}+X_{cs}-X_{Lp})^2 + ((X_{cs}-X_{Lp})X_{Ls} + X_{cp}(-X_{cs}+X_{Lp}+X_{Ls}))^2)}}{\frac{2R_2\left(X_{cp}^2 X_{Lp} + (X_{cp}+X_{cs}-X_{Lp})^2 X_{Ls}\right)}{Q_L(R2^2(X_{cp}+X_{cs}-X_{Lp})^2 + ((X_{cs}-X_{Lp})X_{Ls} + X_{cp}(-X_{cs}+X_{Lp}+X_{Ls}))^2)} + 1}
$$

Observation made from the equation is that the first term in the numerator and in the denominator are frequency independent. Those terms variation with respect to frequency is very less shown in figure 7.
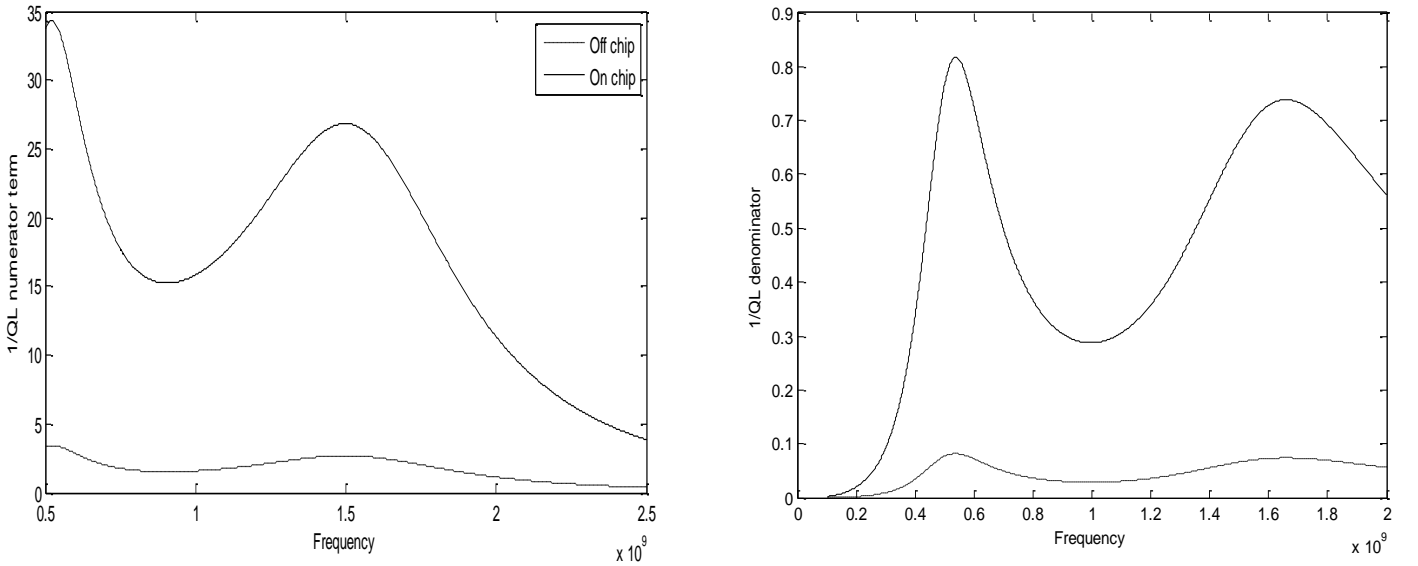

Fig 4.5: Real impedance term varies with frequency

In Zreal equation, the terms which are less effected by QL are neglected. Hence landed with simplified expression for Zreal (11). The simplified and complete expression are compared in on-chip case as well as in off-chip case. The comparison plots are shown in figure 8. Off-chip case the simplified equation is exactly giving the same results as the complete equation. It means the terms which are neglected Zreal equation are less prominent.
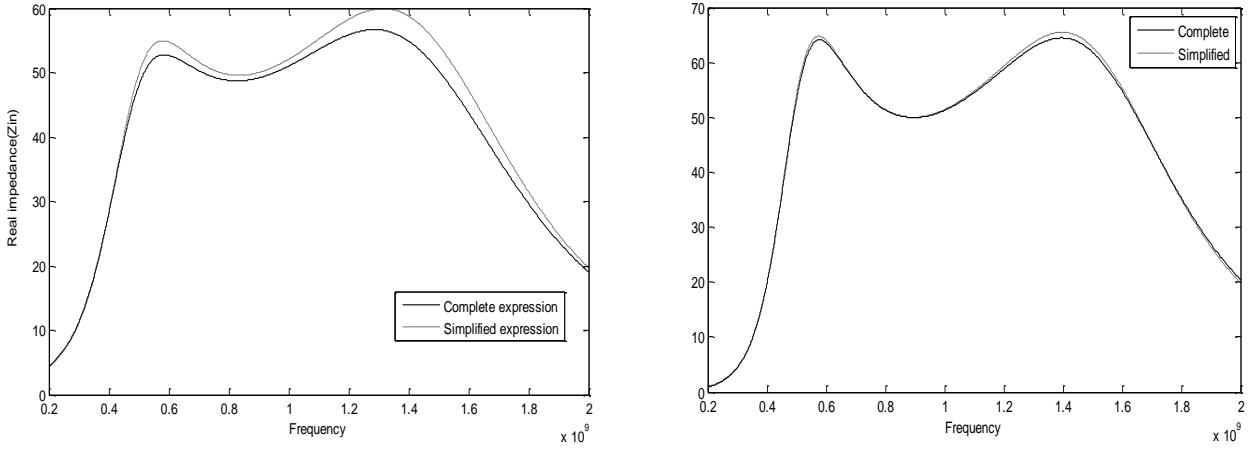
Fig 4.6: Comparision of simplified and complete expression

Imaginary impedance equation is

$$Z_{imag}$$

$$= \frac{\begin{matrix} X_{Lp}(Q_L{}^2(-X_{cp}X_{cs} + Q_L R_2(X_{cp} + X_{cs}) + 2(X_{cp} + X_{cs})X_{Ls})(Q_L R_2(X_{cp} + X_{cs} - X_{Lp}) + \\ X_{cp}X_{Lp} + (X_{cp} + X_{cs} - 2X_{Lp})X_{Ls})(Q_L(Q_L X_{cp}X_{cs} + R_2(X_{cp} + X_{cs})) - \\ (-1 + Q_L{}^2)(X_{cp} + X_{cs})X_{Ls})(Q_L R_2 X_{Lp} + X_{Lp}X_{Ls} + \\ Q_L{}^2((X_{cs} - X_{Lp})X_{Ls} + X_{cp}(-X_{cs} + X_{Lp} + X_{Ls}))))) \end{matrix}}{\begin{matrix} (Q_L{}^2(Q_L R_2(X_{cp} + X_{cs} - X_{Lp}) + X_{cp}X_{Lp} + (X_{cp} + X_{cs} - 2X_{Lp})X_{Ls})^2 \\ + (Q_L R_2 X_{Lp} + X_{Lp}xls + Q_L{}^2((X_{cs} - X_{Lp})X_{Ls} + X_{cp}(-X_{cs} + X_{Lp} + X_{Ls})))^2) \end{matrix}}$$

Parasitic effect of capacitor is not much prominent, hence not considered in the load impedance equation.
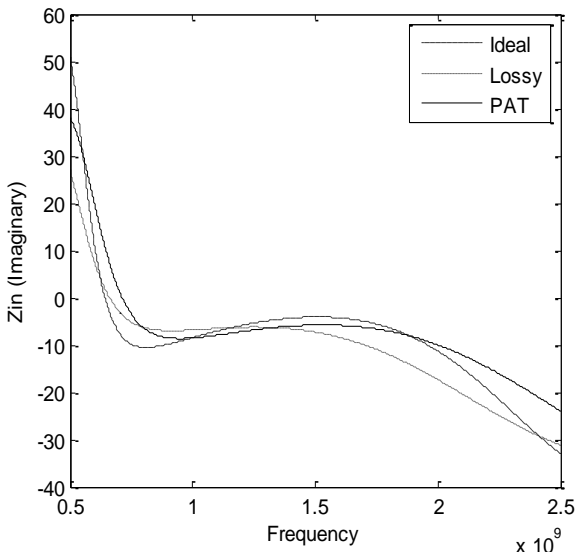
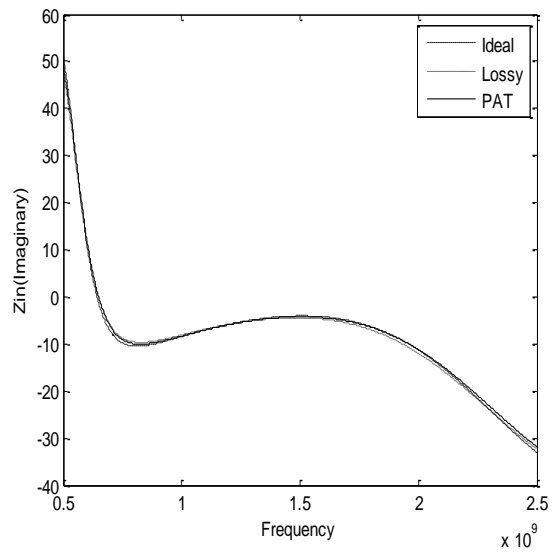Fig 4.7a: Imaginary impedance for on-chip

(QL=5)

Fig 4.7b: Imaginary impedance for off-chip
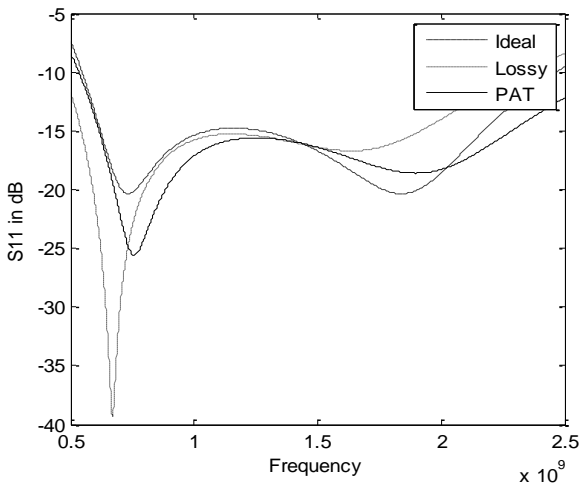
(QL=50)

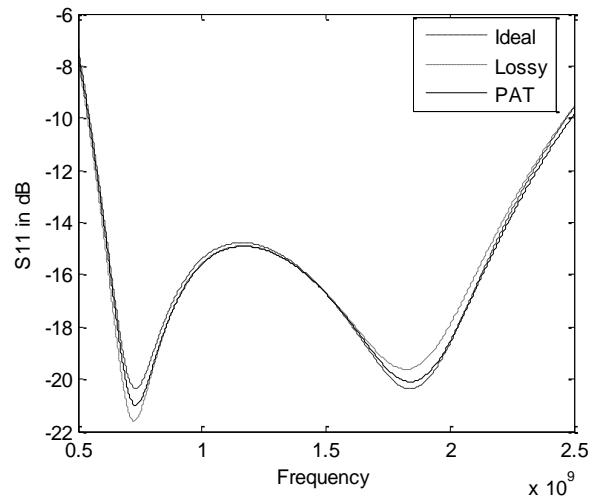Fig 4.8a: S11 plot for on-chip case(QL=5,Qc=30)

Fig 4.8b: S11 plot for off-chip
case(QL=50,Qc=100)

Reflection co-efficient S11 plot for on-chip and off-chip are shown in fig 10. the conclusion drawn from s11 plot is that the impact of component parasitic in broadband matching is less compared to narrowband.

42

4.2.2 Cascade of three L-section

The output of highpass network is given as input to lowpass network and its output is given to second highpass network as input. The source impedance R1 is matched to intermediate impedance Ri1, which lies between highpass and lowpass. The Ri1 is matched to intermediate impedance Ri2, and this Ri2 is matched to load impedance R2, as shown in figure.

Matching to intermediate resistance will lead to low Q. Hence broader bandwidth.
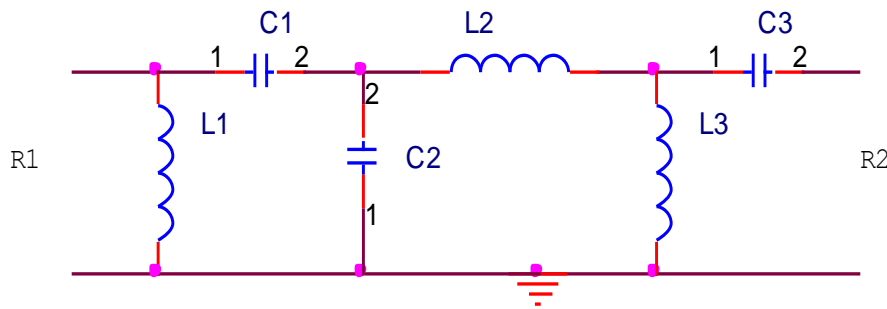

Fig 4.9: Cascade of three LC- sections

The condition for this network is $R1 > Ri1 > Ri2 > R2$

The real impedance equation is given as,

$Zreal$

$$= \frac{\frac{p}{Q_L} + R2xc2^2xL1xL3^2}{\frac{2R2xL3\left(\left(xc1(xc2 - xL2) + xL1xL2 - xc2(xL1 + xL2)\right)^2 + (xc2^2xL1 + (xc1 + xc2 - xL1)^2xL2)xL3\right)}{Q_L} + q} \quad (79)$$

p

$$= \begin{array}{c}(xc1^2(xc3(-xc2 + xL2) + (xc2 + xc3 - xL2)xL3)^2 + 2xc1xc2(xc3(-xc2 + xL2) + (xc2 + xc3 - xL2)xL3) \\ (-xL2xL3 + xc3(xL2 + xL3)) + R2^2(-2xc1xc2(xc2 - xL2 - xL3)(xL2 + xL3) + xc1^2(-xc2 + xL2 + xL3)^2 + \\ xc2^2(xL2 + xL3)(xL1 + xL2 + xL3)) + xc2^2(xL2(xL1 + xL2)xL3^2 - 2xc3xL2xL3(xL1 + xL2 + xL3) \\ + xc3^2(xL2 + xL3)(xL1 + xL2 + xL3)))\end{array}$$

43

q

$$= \frac{(-xL1(-xL2xL3 + xc3(xL2 + xL3)) + xc1(-xL2xL3 + xc2(-xc3 + xL3) + xc3(xL2 + xL3)) + xc2(-(xL1 + xL2)xL3^2}{+xc3(xL1 + xL2 + xL3)))})$$

Z_{real}

$$= \frac{QL(55.73 + QL(131.41 + QL(159.24 + QL(169.75 + QL(89.30 + 49.99QL)))))}{0.155 + QL(0.50 + QL(3.71 + QL(3.51 + QL(4.12 + QL(2.41 + 1.QL)))))} \quad (80)$$

$$Z_{real} = \frac{\dfrac{55.73}{Q_L{}^5} + \dfrac{131.41}{Q_L{}^4} + \dfrac{159.24}{Q_L{}^3} + \dfrac{169.75}{Q_L{}^2} + \dfrac{89.30}{Q_L} + 49.99}{\dfrac{0.155}{Q_L{}^6} + \dfrac{0.50}{Q_L{}^5} + \dfrac{3.71}{Q_L{}^4} + \dfrac{3.51}{Q_L{}^3} + \dfrac{4.12}{Q_L{}^2} + \dfrac{2.41}{Q_L} + 1}$$
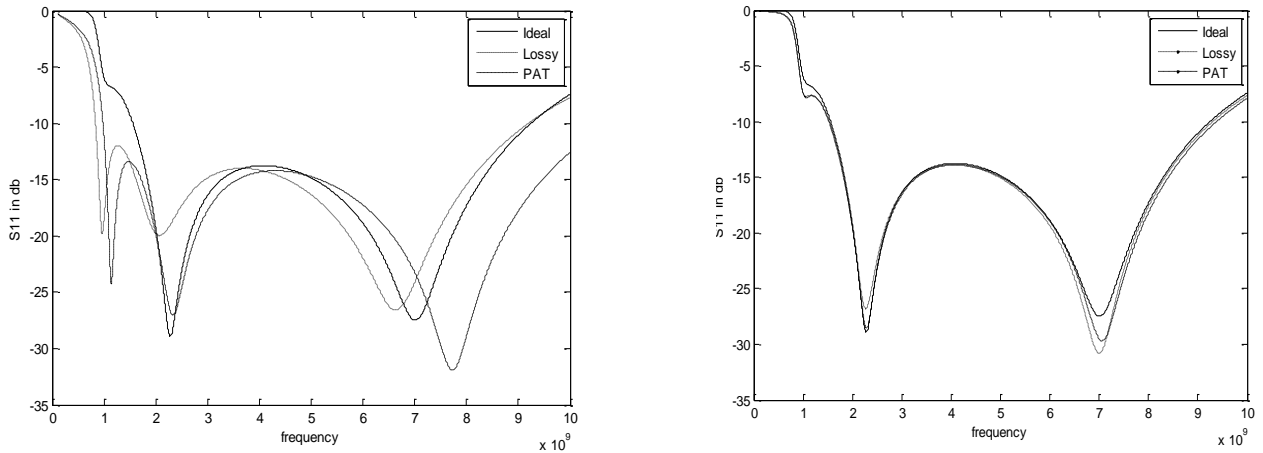
Those terms impact will be less on impedance.

Fig 4.10 : S11 plot for cascade of three L-section in On-chip and off-chip case

4.3 Filter design approach

The improvement in the matching performance from the parasitic aware technique is less compared to narrow band matching shown in fig 16.

The real impedance equation,

$$z_{real}$$

$$= \frac{xcp^2x_{Lp}\left(R_2x_{Lp} + \frac{x_{Ls}(x_{Lp} + x_{Ls})}{Q_L^3} + \frac{R_2(x_{Lp} + 2x_{Ls})}{Q_L^2} + \frac{\left(R_2^2 + x_{cs}^2 - 2x_{cs}x_{Ls} + x_{Ls}(x_{Lp} + x_{Ls})\right)}{\square_\square}\right)}{\begin{array}{c}((R_2^2 + (xcp + xcs)^2)xLp^2 - \\ 2x_{Lp}(-xcp^2 + (x_{cp} + x_{cs})x_{Lp})x_{Ls} +\end{array}}$$

$$\frac{2R_2xLp^2x_{Ls}}{Q_L^3} + \frac{xLp^2xLs^2}{Q_L^4} + \frac{2R_2(xcp^2x_{Lp} + (x_{cp} - x_{Lp})^2x_{Ls})}{\square_\square} + \frac{(xcp^2 - 2x_{cp}x_{Lp} + 2xLp^2)xLs^2)}{Q_L^2}$$

$$+ \left(R_2^2(x_{cp} - x_{Lp})^2 + \left(x_{Lp}(x_{cs} - x_{Ls}) + x_{cp}(-x_{cs} + x_{Lp} + x_{Ls})\right)^2\right)$$

$$Zreal = \frac{QL(269.05 + QL(169.8 + QL(183.4 + 49.95QL)))}{14.36 + QL(11.73 + QL(12.07 + QL(5.37 + 1.QL)))}$$

4.4 Impedance inverting technique (Norton transform)

Once we design a bandpass filter with *Rin_eq* terminated at both the ends, *Rin_eq* at the input side should be transferred to *Zs* with an impedance inverter as shown in Figure 13.
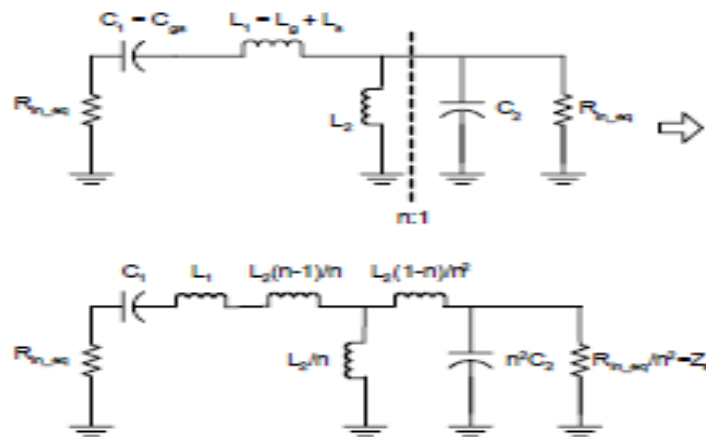

Fig 4.11: Replacing an inductor with three inductors using Norton transform

Freq fH=5G, fL=0.7G	L1 (nH)	L2 (nH)	L3 (nH)	C1 (pF)	C2 (pF)
Ideal	0.36	11.5	-3.52	0.17	3.35
QL=50, QC=100	0.37	11.8	-3.60	0.17	3.46
QL=5,QC=30	0.29	9.34	-2.84	0.21	3.72

Step 1: Matching source impedance R1 to load impedance R2 using Lowpass network at w0

$$w0 = \sqrt{wH \; wL}$$

Where wH=upper frequeny, wL=Lower frequency

Step 2: Transform lowpass to bandpass by replacing inductor to series LC and capacitor to parallel LC. Calculate the transformed values using PAT.

Step 3: Replace parallel inductor L2 with three inductor

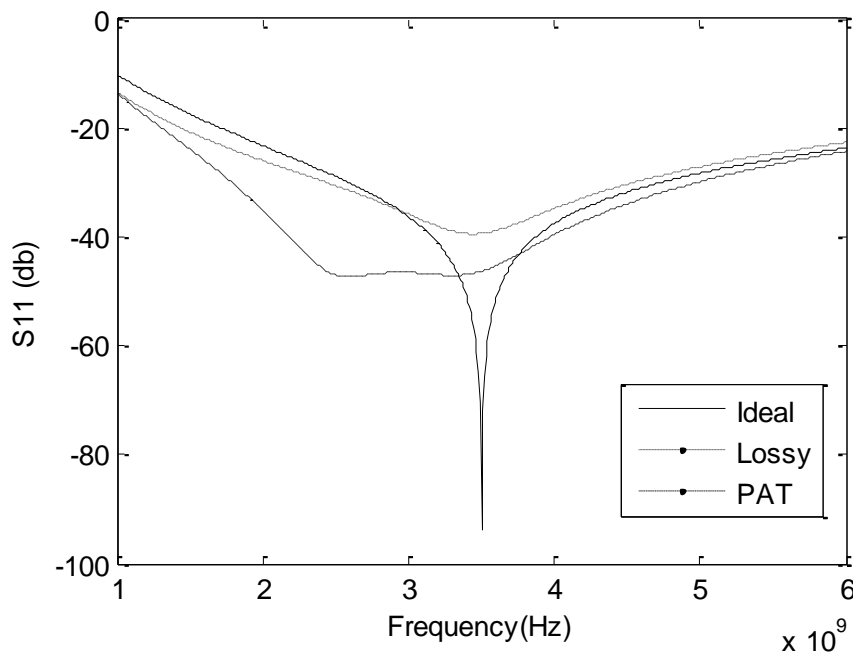L3=L2 (n-1)/n   L1=L2 (1-n)/n^2 L2=L2/n

Fig 4.12: S11 plot of Norton transformed network

Since we addressed *Rin_eq* to be smaller than *Zs*, inverting factor *n* in Figure 13 is less than unity, so that the inductance *L2(n-1)/n*, which is connected to *L1* in series, is a negative value resulting in a smaller gate inductance *Lg*. In general, *Rin_eq* is not very small when compared to *Zs*, thus *n* is very close to unity according to the definition *in eq s n R Z _ = .* As a result, the other series inductor, *L2(1-n)/n2*, becomes small enough to be implemented either as a simple line in the layout or as a bonding wire.

4.5 Analysis of parasitic impact on Asymmetrical filters

The use of asymmetrical bandpass LC filters as input matching networks for wideband impedance matching allows simpler structures for the matching of unequal resistances, some voltage gain and stronger attenuation at high frequency.

In this section the parasitic impact on matching performance for asymmetrical networks is investigated[ ].
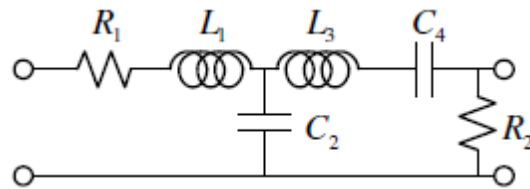

Fig 4.13: Second order asymmetric filter

The real impedance equation is given by

$$Z_{real} = \frac{xL1}{Q_L} + \frac{xc2^2(R_2 + \frac{xL3}{Q_L})}{(R2^2 + (xc2 + xc4 - xL3)^2) + \frac{2R2xL3}{Q_L} + \frac{xL3^2}{Q_L^2}}$$

The imaginary equation,

$$Z_{imag} = xL1 - \frac{xc2((xc4 - xL3)(xc2 + xc4 - xL3) + (R2 + \frac{xL3}{QL})^2)}{(xc2 + xc4 - xL3)^2 + (R2 + \frac{xL3}{QL})^2}$$
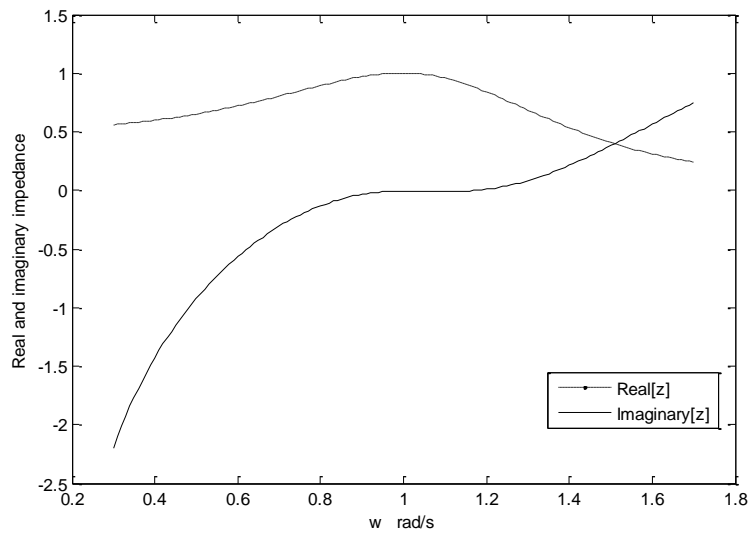

Fig 4.14: Real and imaginary impedance plot

The effect of parasitic on broadband matching using asymmetrical network are less is verified by considering an example. Assume values are normalized by w. Let R1=1ohm and R2=2 ohm. The Zreal expression is given by,

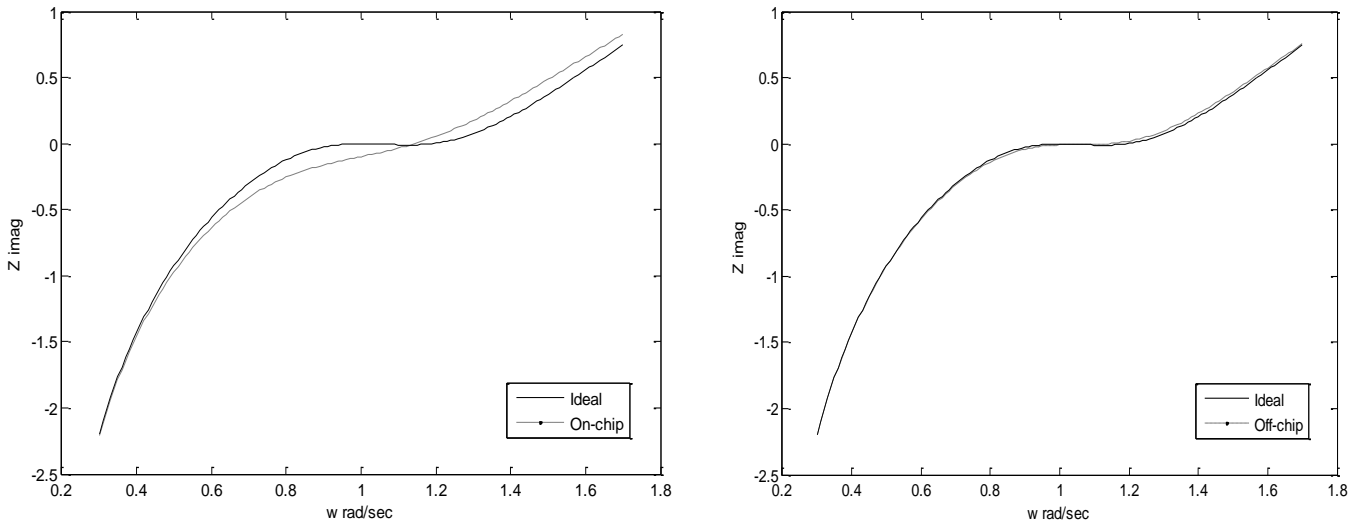$$Z_{real} = \frac{1.098}{QL} + \frac{0.99QL(1.09 + QL)}{0.99 + QL(1.81 + 1.QL)}$$
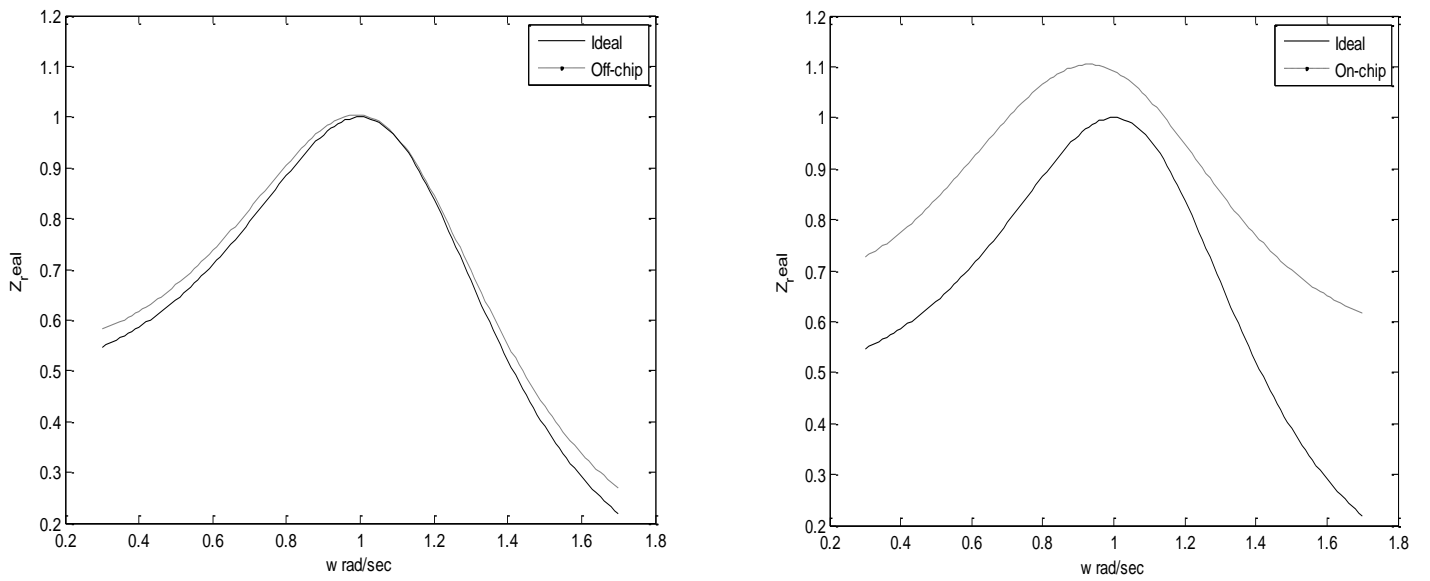
48

Fig 4.15: Imaginary impedance plot

Fig 4.16: Real impedance plot

The QL terms whose effect is less are removed frrom z_real equation. The simplified equation is shown in

$$Z_{real} = \frac{xc2^2(R_2 + \frac{xL3}{Q_L})}{(R2^2 + (xc2 + xc4 - xL3)^2) + \frac{2R2xL3}{\square_\square}}$$
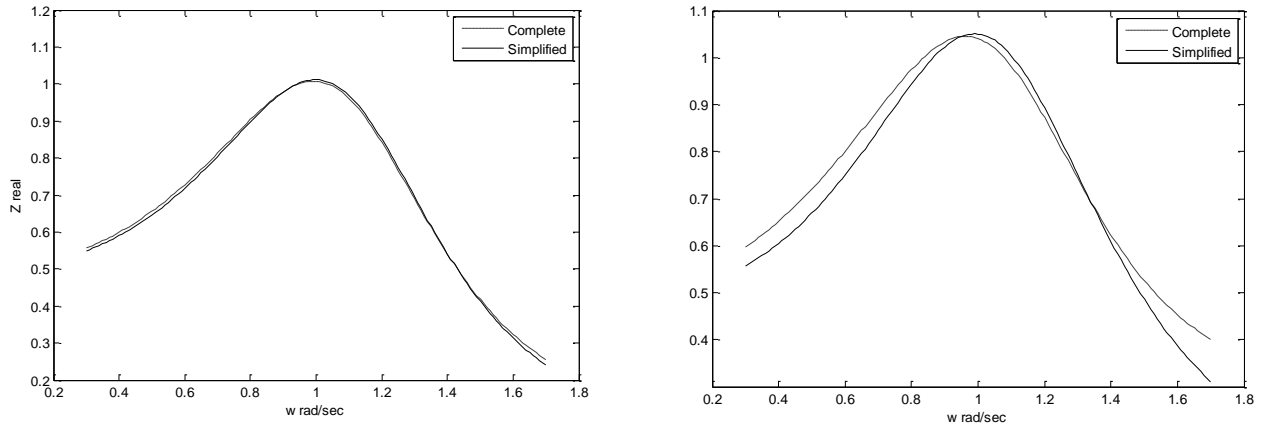

Fig 4.17: Complete and simplified impedance equation

The z_real equation can be simplified to

$$Z_{real} = \frac{xc2^2 R_2}{R2^2 + (xc2 + xc4 - xL3)^2}$$

4.4 Conclusion

The observation from the analysis on broadband impedance matching network is that, the impact of component parasitic are less compared to narrow band impedance matching.

.

5. Conclusion and Future work

5.1 Conclusion

This thesis proposed two methods, Equivalent Impedance method and Parasitic Absorption method, for designing concurrent multi-band L-matching networks including the component non-idealities. Both methods show better performance in terms of matching quality and frequency even with low quality factor components. Also the proposed methods were validated in practical environment for different impedances and on-chip and off-chip cases. These design methods are also extended for quad band matching. The proposed method can extended for broadband matching network design in future.

In this document a new methodology for designing Broadband impedance matching network as been proposed. From this technique a flat band can be obtained. Band can be stretched for given input reflection coefficient. Also the impact of component parasitic of broadband impedance matching network is analyzed and showed that the impact is less compared to narrowband.

5.2 Future Work

- PCB of the, Dual band impedance matching network and broadband matching network.
- Analysis of parasitic impact on all broadband impedance matching network

References

[1] Youssef, M.; Zolfaghari, A.; Mohammadi, B.; Darabi, H.; Abidi, A.A., "A
[1]Low-Power GSM/EDGE/WCDMA Polar Transmitter in 65-nm CMOS," Solid-State Circuits, IEEE Journal of , vol.46, no.12, pp.3061,3074, Dec. 2011

[2] Oliaei, O.; Kirschenmann, M.; Newman, D.; Hausmann, K.; Haolu Xie; Rakers, P.; Rahman, M.; Gomez, M.; Chuanzhao Yu; Gilsdorf, B.; Sakamoto, K., "A multiband multimode transmitter without driver
amplifier," Solid-State Circuits Conference Digest of Technical Papers (ISSCC), 2012 IEEE International , vol., no., pp.164,166, 19-23 Feb. 2012

[3] Cassia, M.; Hadjichristos, A.; Hong Sun Kim; Jin-Su Ko; Jeongsik Yang; Sang-Oh Lee; Sahota, G., "A Low-Power CMOS SAW-Less Quad Band WCDMA/HSPA/HSPA+/1X/EGPRS Transmitter," Solid-State Circuits, IEEE Journal of , vol.44, no.7, pp.1897,1906, July 2009

[4] Kaczman, D.L.; Shah, M.; Godambe, N.; Alam, M.; Guimaraes, H.; Han, L.M.; Rachedine, M.; Cashen, D.L.; Getka, W.E.; Dozier, C.; Shepherd, W.P.; Couglar, K., "A single-chip tri-band (2100, 1900, 850/800 MHz) WCDMA/HSDPA cellular transceiver," Solid-State Circuits, IEEE Journal of , vol.41, no.5, pp.1122,1132, May 2006

[5] Parssinen, A., "Multimode-multiband transceivers for next generation of wireless communications," Solid-State Device Research Conference (ESSDERC), 2011 Proceedings of the European , vol., no., pp.42,53, 12-16 Sept. 2011

[6] Hashemi, H.; Hajimiri, A., "Concurrent multiband low-noise amplifierstheory, design, and applications," Microwave Theory and Techniques, IEEE Transactions on , vol.50, no.1, pp.288,301, Jan 2002

[7] N. M. Neihart, J. Brown, and X. Yu, "A dual-band 2.45/6 GHz CMOS LNA utilizing a dual-resonant transformer-based matching network," IEEE Trans. Circuits Syst. I, Reg. Papers, vol. 59, no. 8, pp. 17431751, Aug. 2012.

[8] Kai-An Hsieh; Hsien-Shun Wu; Kun-Hung Tsai; Tzuang, C.-K.C., "A Dual-Band 10/24-GHz Amplifier Design Incorporating Dual-Frequency Complex Load Matching," Microwave Theory and Techniques, IEEE Transactions on , vol.60, no.6, pp.1649,1657, June 2012

[9] Nieuwoudt, A.; Ragheb, T.; Nejati, H.; Massoud, Y., "Numerical Design Optimization Methodology for Wideband and Multi-Band Inductively Degenerated Cascode CMOS Low Noise Amplifiers," Circuits and Systems I: Regular Papers, IEEE Transactions on , vol.56, no.6, pp.1088,1101, June 2009

[10] C. Bowick, RF Circuit Design. London, U.K.: Howard W. Sams, 1985. [11] T. H. Lee, "Design of CMOS Radio-Frequency Integrated Circuits," 2nd ed., Cambridge University Press, 2004.

[12] Becciolini, B. (1993), "Motorola application note: Impedance matching networks applied to RF power transistors," http://www.rfwireless.rell.com/pdfs/AN 721 D.pdf.

[13] Nallam, N.; Chatterjee, S., "Multi-Band Frequency Transformations, Matching Networks and Amplifiers," Circuits and Systems I: Regular Papers, IEEE Transactions on , vol.60, no.6, pp.1635,1647, June 2013

[14] Jinho Park, Kiyong Choi, and Allstot, D.J., "Parasitic-aware RF circuit design and optimization," Circuits and Systems I: Regular Papers, IEEE Transactions on , vol.51, no.10, pp.1953,1966, Oct. 2004

[15] Van Bezooijen, A.; De Jongh, M.A.; van Straten, F.; Mahmoudi, R.; Van Roermund, A. H M, "Adaptive Impedance-Matching Techniques for Controlling L Networks," Circuits and Systems I: Regular Papers, IEEE Transactions on , vol.57, no.2, pp.495,505, Feb. 2010

[16] Po, F.C.W.; De Foucauld, E.; Morche, D.; Vincent, P.; Kerherve, E., "A Novel Method for Synthesizing an Automatic Matching Network and Its Control Unit," Circuits and Systems I: Regular Papers, IEEE Transactions on , vol.58, no.9, pp.2225,2236, Sept. 2011

[17] Qizheng Gu; Morris, A.S., "A New Method for Matching Network Adaptive Control," Microwave Theory and Techniques, IEEE Transactions on , vol.61, no.1, pp.587,595, Jan. 2013

[18] Soltani, N.; Fei Yuan, "A High-Gain Power-Matching Technique for Efficient Radio-Frequency Power Harvest of Passive Wireless Microsystems," Circuits and Systems I: Regular Papers, IEEE Transactions on , vol.57, no.10, pp.2685,2695, Oct. 2010

[19] Bing Jiang; Smith, J.R.; Philipose, M.; Roy, S.; Sundara-Rajan, K.; Mamishev, A.V., "Energy Scavenging for Inductively Coupled Passive RFID Systems," Instrumentation and Measurement, IEEE Transactions on , vol.56, no.1, pp.118,125, Feb. 2007

[20] K. Dasgupta, A. Dutta and T. K. Bhattacharya, "Parasitic Aware Impedance Matching Technique for RF Amplifiers," Analog Integrated Circuit Signal Processing, 70:91-102, 2012.

[21] Becciolini, B. (1993), "Motorola application note: Impedance matching networks applied to RF power transistors,"
http://www.rfwireless.rell.com/pdfs/AN 721 D.pdf.

[22] H.J.Lee and Dong Sam Ha," A Systematic Approach to CMOS Low Noise Amplifier Design for Ultrawideband Applications.